Exact Green's function approach to RKKY interactions

Tomasz M. Rusin [*] and Wlodek Zawadzki
Institute of Physics, Polish Academy of Sciences, Al. Lotników 32/46, 02-688 Warsaw, Poland

(Received 1 February 2020; accepted 1 April 2020; published 1 May 2020)

The Green's function (GF) of two localized magnetic moments embedded in the electron gas is calculated exactly. The electrons are treated in the effective mass approximation and the magnetic moments are coupled with electrons by a deltalike *s*-*d* interaction. The resulting GF is obtained as a result of the exact summation of the Born series using a generalization of the method developed by Slater-Koster and Ziman to noncommuting spin operators with the use of the Woodbury identities. For small *s*-*d* coupling J the exact GF reduces to the Ruderman-Kittel-Kasuya-Yosida (RKKY) case, for which the first two terms of the Born series are included. In contrast to the standard RKKY, for the exact GF there is no symmetry between positive and negative values of J. The exact GF crucially depends on the value of the one-electron Green's function at the origin, denoted as g_0. The Born series is convergent only if g_0 is finite, which holds for electrons in parabolic energy bands in one dimension, but not in two and three dimensions. For this reason, a simple model of RKKY interaction deserves to be reconsidered since the second term of the perturbation series is finite, and gives the standard RKKY interaction, while the sum of remaining terms is divergent. A finite value of g_0 can be obtained once a cutoff for the energy integration is introduced. The exact GF includes nonlinear combination of localized spin operators and a method of calculating matrix elements of these operators is given. For spins $\hat{S}_a, \hat{S}_b = \frac{1}{2}$ the exact GF is expressed as a linear combination of components of $\hat{S}_a, \hat{S}_b$, and the exact range function $\mathcal{J}(r_{ab})$ is obtained as a double integral over analytical expression. For electron energy $E = 0$ and $Jg_0/2 \simeq 2$ or $Jg_0/2 \simeq -\frac{2}{3}$, the range function and GF are singular. Poles of GF occur in the vicinities of singularity points and the resulting energies of bound states are calculated. The origin of asymmetry between positive and negative J values is explained. For small $|J|$ the range function $\mathcal{J}(r_{ab})$ resembles the RKKY one: it has the same period π/k_F, the same decay character, and a slightly different amplitude, usually within a few percent. This regime occurs most frequently in the nature. For $|J|$ comparable to $|g_0|^{-1}$, the exact range function has much larger amplitude and nonoscillatory character. For $|J| \gg |g_0|^{-1}$, the exact range function oscillates with the same period and powerlike decay as the usual RKKY function but it has much lower amplitude decaying with growing $|J|$. In the limiting case of $|J| \to \infty$, the range function vanishes. A range of validity of the proposed model to real systems is discussed.

DOI: 10.1103/PhysRevB.101.205201

I. INTRODUCTION

In 1954 Ruderman and Kittel described interaction between nuclear magnetic moments of impurities in metals [1]. The interaction was mediated by conduction electrons and had a long-range character. It was found that the second-order correction to the energy of free-electron gas due to the presence of two nuclei is proportional to the product of the two spin operators and the range function $\mathcal{J}_{\rm RK}(r_{ab})$ depended on the distance r_{ab} between spins. The range function oscillates in space with the period π/k_F, where k_F is the Fermi vector, and for large distances it decays as $1/r_{ab}^3$. Sometime later, Kasuya [2] and Yoshida [3] pointed out that exactly the same interaction appears between magnetic atom impurities in metals as a result of *s*-*d* or *s*-*f* hybridization.

During the last 60 years the Ruderman-Kittel-Kasuya-Yosida (RKKY) interaction was investigated both theoretically and experimentally in more realistic systems. The review works of RKKY can be found in Ref. [4] and many textbooks of solid state physics (see [5]).

In this paper we propose a method of exact summation of the Born series for two localized spins interacting with electron gas by the *s*-*d* interaction. Our calculations generalize the RKKY theory by taking into account all terms of perturbation series instead of retaining only terms of the second order in the *s*-*d* coupling constant J. We calculate the exact Green's function (GF) of the system using a modification of the method proposed by Slater-Koster-Ziman to potentials including noncommuting spin operators [6]. Having calculated the exact GF of the system we clarify the issues of convergence of Born series and calculate the range function obtained from the exact GF. We also clarify the issues related to behavior of GF and the range function for small and large values of $|J|$ and discuss the possibility of existence of localized states. It appears that these results have not been reported in literature.

Our intention is to compare the exact results with those obtained for standard RKKY theory. For this reason we consider electrons in parabolic energy bands described by the effective mass approximation. Within this approach we calculate the impact of higher-order terms of the Born series on the GF and range function of RKKY problem. We mostly concentrate on the three-dimensional (3D) case at $T = 0$.

---

[*] tmr@vp.pl

The paper is organized as follows. Section II outlines the derivation of RKKY using the second-order terms of the Born series and discusses some properties of singular potentials. Section III introduces the Dyson equation of the problem and its solution with use of Woodbury identities. In Sec. IV we express the exact GF for arbitrary spins as nonlinear combination of localized spin operators. Section V provides a method of calculating matrix elements of exact GF in Sec. IV. Section VI considers the case of spins $\hat{S}_a, \hat{S}_b = \frac{1}{2}$ and expresses the exact GF as a linear function of products of spin operators. Section VII contains calculations of density of states obtained from the exact GF, the grand canonical potential depending on localized spin configuration and the corresponding range function. Section VIII introduces a simplified model of exact GF, grand canonical potential, and the range function valid for fast-decaying one-electron GF. This approximation allows us to understand the physical origin of several peculiarities existing in the exact results. Section IX discusses one-electron GF used in further calculations and introduces an energy cutoff for one-electron GF at the origin. Section X contains numerical calculations of the exact range function for several values of key model parameters. In Sec. XI we discuss our results. The work is concluded by the Summary. Appendices and Supplemental Material [7] provide auxiliary information related to the problems analyzed in this work.

II. PRELIMINARIES

Let us consider the Dyson equation $\hat{G} = \hat{g} + \hat{g}\hat{V}\hat{G}$, where $\hat{V} = \hat{V}_a + \hat{V}_b$, $\hat{V}_a$ and $\hat{V}_b$ are two nonoverlapping potentials, $\hat{g}$ is the GF in absence of $\hat{V}$, and $\hat{G}$ is the GF in the presence of $\hat{V}$. Iterating the Dyson equation one obtains the Born series $\hat{G} \simeq \hat{g} + \hat{g}\hat{V}\hat{g} + \hat{g}\hat{V}\hat{g}\hat{V}\hat{g} + \cdots$. The lowest-order terms of this series depending on both $\hat{V}_a$ and $\hat{V}_b$ are

$$\hat{G}^{ab} \simeq \hat{g}\hat{V}_a\hat{g}\hat{V}_b\hat{g} + \hat{g}\hat{V}_b\hat{g}\hat{V}_a\hat{g} + \cdots . \tag{1}$$

We consider the potentials $\hat{V}_c$ with $c = a, b$ in the form of contact *s*-*d* interaction

$$\hat{V}_c(\boldsymbol{r}) = J\delta(\boldsymbol{r} - \boldsymbol{r}_c)\hat{\boldsymbol{S}}_c\hat{\boldsymbol{s}}, \tag{2}$$

where J is the *s*-*d* coupling constant measured in $J \times m^D$ units, D is system dimensionality, $\hat{\boldsymbol{s}} = \boldsymbol{\sigma}/2$ is the electron spin operator, and $\boldsymbol{\sigma}$ are the Pauli matrices in the standard notation. The operators $\hat{\boldsymbol{S}}_c$ describe localized spins of atomic nuclei or magnetic impurities. Taking the trace of $\hat{G}^{ab}$ one finds the density of states (DOS) of the system $n(E)$ and the corresponding thermodynamic potential $\Omega[n(E)]$. For the one-electron Green's function $\hat{g}$ in the effective mass approximation, $D = 3$ and $T = 0$ one obtains the well-known result [1]

$$\Delta\Omega \simeq \mathcal{J}_{\rm RK}\hat{\boldsymbol{S}}_a\hat{\boldsymbol{S}}_b, \tag{3}$$

$$\mathcal{J}_{\rm RK}(r_{ab}) = \frac{J^2}{64\pi^3 r_{ab}^4\zeta}[2r_{ab}k_F\cos(2k_F r_{ab}) - \sin(2k_F r_{ab})], \tag{4}$$

where $\zeta = \hbar^2/(2m^*)$, k_F is the Fermi vector, m^* is electron effective mass, and r_{ab} is the distance between $\hat{S}_a$ and $\hat{S}_b$. Equations (3) and (4) describe the RKKY Hamiltonian and range function of electrons interacting with localized spins. The RKKY interaction in Eq. (4) is of second-order effect in terms of *s*-*d* coupling constant J.

There appear questions about the validity of Eqs. (3) and (4). First, about the convergence of the Born series and the impact of remaining infinite number of terms on the range function in Eq. (4). Next, one may ask whether the Born series converges for arbitrary J or is there a critical value of J above which the perturbation series diverges. Finally, is it possible that for sufficiently large $|J|$ there appear localized or resonant states.

Taking proper material band structure, reasonable physical parameters, and including other effects appearing in solids (as, e.g., phonons, disorder, many-body effects in electron gas and in ion electrons), the RKKY theory correctly describes experimental results [4]. This implies that for the RKKY problem, the Born series converges and its higher-order terms do not alter significantly the results in Eqs. (3) and (4). Another implication is that even if there is a critical value of J leading to divergence of the Born series, its magnitude is much larger than $|J|$ observed in real materials.

However, there are at least three hints indicating that the impact of higher-order terms in the Born series is more complicated and ambiguous. First, as pointed in Refs. [8,9], the third-order term of the perturbation series for RKKY energy is divergent. However, there exists a suggestion of Kittel that, possibly the whole Born series is convergent irrespective of the fact that some of its terms diverge if calculated separately [10]. The second hint is that taking into account only spin parts of the potentials $\hat{V}_a$ and $\hat{V}_b$, the higher-order terms are more complicated functions of localized spins in Eq. (3). The last hint relates to analytical results obtained for the case of single scalar deltalike potential. Let $\hat{V}_b = 0$ and $\hat{V}_a = v_a\delta(\boldsymbol{r} - \boldsymbol{r}_a)$, where v_a is potential strength. Using the method proposed by Slater, Koster, Ziman, and others [6,11–13] one can sum the Born series to obtain

$$G(\boldsymbol{r}_1, \boldsymbol{r}_2) = g(\boldsymbol{r}_1, \boldsymbol{r}_2) + g(\boldsymbol{r}_1, \boldsymbol{r}_a)\frac{v_a}{1 - g_0 v_a}g(\boldsymbol{r}_a, \boldsymbol{r}_2), \tag{5}$$

where $g_0 = g(\boldsymbol{r}_a, \boldsymbol{r}_a)$ is one-electron GF at the origin. The GF in Eq. (5) exists only when the quantity g_0 is finite. For $|g_0 v_a| \ll 1$ one may neglect $|g_0 v_a|$ in the denominator of Eq. (5) and the GF is well approximated by its lowest-order terms in v_a. By increasing $|g_0 v_a|$ the corrections due to the denominator in Eq. (5) are more pronounced. For vanishing imaginary part of g_0 and appropriate value of v_a there appears a pole of GF, indicating an existence of localized states. For $|g_0 v_a| \gg 1$ the second term in Eq. (5) gradually decreases and for $v_a \to \infty$ the GF does not depend on v_a. Finally, the GF in Eq. (5) is not symmetric for positive and negative values of v_a.

The above hints suggest that the RKKY interaction obtained in a second order of perturbation expansion, as given in Eqs. (3) and (4), may overlook some important properties of the system. The potentials $\hat{V}_a$ and $\hat{V}_b$ are products of deltalike potentials and spin interactions between conduction electrons and localized moments. Therefore, the true GF of the system should include spin effects, e.g., its dependence on relative spin orientations and effects related to deltalike potentials, similar to those following from Eq. (5).

III. GREEN'S FUNCTION OF THE SYSTEM

We consider the electron gas perturbed by two localized spins $\hat S_a$, $\hat S_b$ placed in $\boldsymbol r_a$, $\boldsymbol r_b$, respectively. The potential of the *s*-*d* interaction between the spins and the electron gas is

$$\hat V(\boldsymbol r) = \hat{\boldsymbol Z}_a \delta(\boldsymbol r - \boldsymbol r_a) + \hat{\boldsymbol Z}_b \delta(\boldsymbol r - \boldsymbol r_b) \equiv \hat V_a + \hat V_b, \tag{6}$$

where we defined $\hat{\boldsymbol Z}_a = J\hat{\boldsymbol S}_a \hat{\boldsymbol s}/2$ and $\hat{\boldsymbol Z}_b = J\hat{\boldsymbol S}_b \hat{\boldsymbol s}/2$ [see Eq. (2)]. Note the sign convention in Eq. (6): positive sign of J corresponds to antiferromagnetic coupling between impurity and electron spins. Then,

$$\hat{\boldsymbol Z}_c = \frac{J}{2}\begin{pmatrix} +\hat S_c^z & \hat S_c^- \\ \hat S_c^+ & -\hat S_c^z \end{pmatrix}, \quad c = a, b. \tag{7}$$

The main differences between the scalar potential in Eq. (5) and the spin-dependent potentials in Eqs. (6) and (7) are (i) the x, y, z components of $\hat V_a$ and $\hat V_b$ do not commute and (ii) the potentials $\hat V_a$ and $\hat V_b$ as given in Eq. (2) do not commute, which can be demonstrated by direct calculations. Then, in further calculation one has to ensure proper order of spin operators and its components. Because of the nonzero commutator of $\hat V_a$ and $\hat V_b$ in Eq. (6), we may not apply the results obtained for the Kondo problem [14,15].

We treat the electron gas in the single-particle approximation and assume that the electron spin is a good quantum number, i.e., the periodic potential of the lattice does not mix electron states of different spins. The one-electron states are then two-component spinors $|\boldsymbol k\nu\rangle = |\boldsymbol k\rangle \times |\nu\rangle$, where $\nu \in \{\uparrow, \downarrow\}$ is the s_z component of electron spin, and $|\boldsymbol k\rangle$ is the Bloch state of the conduction band.

The conduction band is filled by electrons up to the energy E_F and we neglect interactions between electrons. The energy dispersion $\epsilon(\boldsymbol k)$ may be arbitrary, but spin independent. Then, the one-electron Green's function is a 2×2 matrix diagonal in spin variables

$$\hat{\boldsymbol g}(\boldsymbol r_1, \boldsymbol r_2, \nu_1, \nu_2) = g(\boldsymbol r_1, \boldsymbol r_2)\begin{pmatrix} 1 & 0 \\ 0 & 1 \end{pmatrix}, \tag{8}$$

where

$$g(\boldsymbol r_1, \boldsymbol r_2, E) = \sum_{\boldsymbol k} \frac{|\boldsymbol k\rangle\langle \boldsymbol k|}{E - \epsilon_{\boldsymbol k}}. \tag{9}$$

The only assumption for GF in Eq. (9) is that, for all energies $E > 0$, the GF at the origin g_0 is finite and nonzero

$$|g_0| = |\lim_{\boldsymbol r_1 \to \boldsymbol r_2} g(\boldsymbol r_1, \boldsymbol r_2, E)| \in (0, \infty). \tag{10}$$

In Sec. IX we consider the one-electron GF for parabolic energy band in the effective mass approximation, which is a special case of GF in Eq. (9).

A. Dyson equation

Within the model described above we solve the Dyson equation for the exact GF of the system. Let $\hat{\boldsymbol G}$ be the Green's function of the electron gas in the presence of external potential given in Eq. (6). The functions $\hat{\boldsymbol G}$ and $\hat{\boldsymbol g}$ are related to each other by the Dyson equation: $\hat{\boldsymbol G} = \hat{\boldsymbol g} + \hat{\boldsymbol g}V\hat{\boldsymbol G}$. In the position representation there is

$$\hat{\boldsymbol G}_{12} = \hat{\boldsymbol g}_{12} + \int \hat{\boldsymbol g}_{13} V(\boldsymbol r_3) \hat{\boldsymbol G}_{31} d^3\boldsymbol r_3. \tag{11}$$

In Eq. (11) and below we use the notation $\hat{\boldsymbol G}_{12} = \hat{\boldsymbol G}(\boldsymbol r_1, \boldsymbol r_2)$ and $\hat{\boldsymbol g}_{12} = \hat{\boldsymbol g}(\boldsymbol r_1, \boldsymbol r_2)$. Since the potential $V(\boldsymbol r_3)$ in Eq. (6) is the sum of delta functions multiplied by spin operators one obtains

$$\hat{\boldsymbol G}_{12} = \hat{\boldsymbol g}_{12} + \hat{\boldsymbol g}_{1a}\hat{\boldsymbol Z}_a \hat{\boldsymbol G}_{a2} + \hat{\boldsymbol g}_{1b}\hat{\boldsymbol Z}_b \hat{\boldsymbol G}_{b2}, \tag{12}$$

where $\hat{\boldsymbol g}_{12}^{\pm}$, $\hat{\boldsymbol g}_{1a}^{\pm}$, $\hat{\boldsymbol g}_{1b}^{\pm}$ are given in Eqs. (8) and (9). The function $\hat{\boldsymbol G}_{12}$ is a 2×2 matrix and the main objective of this paper is to obtain its four components in the analytical form.

To find $\hat{\boldsymbol G}_{12}$ we generalize the method proposed by Slater-Koster and Ziman to sum the Born series for neutral deltalike impurity embedded in the noninteracting electron gas [6,11–13]. By setting in Eq. (12) $\boldsymbol r_1 \to \boldsymbol r_a$ and $\boldsymbol r_1 \to \boldsymbol r_b$ one obtains two coupled equations for $\hat{\boldsymbol G}_{a2}$ and $\hat{\boldsymbol G}_{b2}$:

$$\hat{\boldsymbol G}_{a2} = \hat{\boldsymbol g}_{a2} + \hat{\boldsymbol g}_{aa}\hat{\boldsymbol Z}_a \hat{\boldsymbol G}_{a2} + \hat{\boldsymbol g}_{ab}\hat{\boldsymbol Z}_b \hat{\boldsymbol G}_{b2}, \tag{13}$$

$$\hat{\boldsymbol G}_{b2} = \hat{\boldsymbol g}_{b2} + \hat{\boldsymbol g}_{ba}\hat{\boldsymbol Z}_a \hat{\boldsymbol G}_{a2} + \hat{\boldsymbol g}_{bb}\hat{\boldsymbol Z}_b \hat{\boldsymbol G}_{b2}. \tag{14}$$

We may rewrite Eqs. (13) and (14) in a matrix form

$$\begin{pmatrix} \hat I - \hat{\boldsymbol g}_{aa}\hat{\boldsymbol Z}_a & -\hat{\boldsymbol g}_{ab}\hat{\boldsymbol Z}_b \\ -\hat{\boldsymbol g}_{ba}\hat{\boldsymbol Z}_a & \hat I - \hat{\boldsymbol g}_{bb}\hat{\boldsymbol Z}_b \end{pmatrix}\begin{pmatrix} \hat{\boldsymbol G}_{a2} \\ \hat{\boldsymbol G}_{b2} \end{pmatrix} = \begin{pmatrix} \hat{\boldsymbol g}_{a2} \\ \hat{\boldsymbol g}_{b2} \end{pmatrix}. \tag{15}$$

In the above equation the matrix is a 4×4 operator. We write formally

$$\begin{pmatrix} \hat{\boldsymbol G}_{a2} \\ \hat{\boldsymbol G}_{b2} \end{pmatrix} = \begin{pmatrix} \hat I - \hat{\boldsymbol g}_{aa}\hat{\boldsymbol Z}_a & -\hat{\boldsymbol g}_{ab}\hat{\boldsymbol Z}_b \\ -\hat{\boldsymbol g}_{ba}\hat{\boldsymbol Z}_a & \hat I - \hat{\boldsymbol g}_{bb}\hat{\boldsymbol Z}_b \end{pmatrix}^{-1}\begin{pmatrix} \hat{\boldsymbol g}_{a2} \\ \hat{\boldsymbol g}_{b2} \end{pmatrix}. \tag{16}$$

To find the matrix in Eq. (16) we consider two 4×4 operators: $\hat{\boldsymbol Y}$ and $\hat{\boldsymbol T} = \hat{\boldsymbol Y}^{-1}$. Let $\hat{\boldsymbol Y}$ be the matrix in Eq. (15),

$$\hat{\boldsymbol Y} = \begin{pmatrix} \hat I - \hat{\boldsymbol g}_{aa}\hat{\boldsymbol Z}_a & -\hat{\boldsymbol g}_{ab}\hat{\boldsymbol Z}_b \\ -\hat{\boldsymbol g}_{ba}\hat{\boldsymbol Z}_a & \hat I - \hat{\boldsymbol g}_{bb}\hat{\boldsymbol Z}_b \end{pmatrix} = \begin{bmatrix} \hat{\boldsymbol A} & \hat{\boldsymbol B} \\ \hat{\boldsymbol C} & \hat{\boldsymbol D} \end{bmatrix}, \tag{17}$$

and $\hat{\boldsymbol T}$ be the matrix in Eq. (16),

$$\hat{\boldsymbol T} = \begin{pmatrix} \hat I - \hat{\boldsymbol g}_{aa}\hat{\boldsymbol Z}_a & -\hat{\boldsymbol g}_{ab}\hat{\boldsymbol Z}_b \\ -\hat{\boldsymbol g}_{ba}\hat{\boldsymbol Z}_a & \hat I - \hat{\boldsymbol g}_{bb}\hat{\boldsymbol Z}_b \end{pmatrix}^{-1} = \begin{pmatrix} \hat{\boldsymbol T}^A & \hat{\boldsymbol T}^B \\ \hat{\boldsymbol T}^C & \hat{\boldsymbol T}^D \end{pmatrix}. \tag{18}$$

In Eq. (18) the operators $\hat{\boldsymbol T}^A, \hat{\boldsymbol T}^B, \hat{\boldsymbol T}^C, \hat{\boldsymbol T}^D$ are undeterminate yet, and they are complicated functions of $\hat{\boldsymbol A}, \hat{\boldsymbol B}, \hat{\boldsymbol C}, \hat{\boldsymbol D}$ (see below). From Eqs. (16) and (18) one has

$$\begin{pmatrix} \hat{\boldsymbol G}_{a2} \\ \hat{\boldsymbol G}_{b2} \end{pmatrix} = \begin{pmatrix} \hat{\boldsymbol T}^A & \hat{\boldsymbol T}^B \\ \hat{\boldsymbol T}^C & \hat{\boldsymbol T}^D \end{pmatrix}\begin{pmatrix} \hat{\boldsymbol g}_{a2} \\ \hat{\boldsymbol g}_{b2} \end{pmatrix}. \tag{19}$$

The exact Green's function in Eq. (12) is

$$\begin{aligned} \hat{\boldsymbol G}_{12} = \hat{\boldsymbol g}_{12} &+ \hat{\boldsymbol g}_{1a}[\hat{\boldsymbol Z}_a \hat{\boldsymbol T}^A]\hat{\boldsymbol g}_{a2} + \hat{\boldsymbol g}_{1a}[\hat{\boldsymbol Z}_a \hat{\boldsymbol T}^B]\hat{\boldsymbol g}_{b2} \\ &+ \hat{\boldsymbol g}_{1b}[\hat{\boldsymbol Z}_b \hat{\boldsymbol T}^C]\hat{\boldsymbol g}_{a2} + \hat{\boldsymbol g}_{1b}[\hat{\boldsymbol Z}_b \hat{\boldsymbol T}^D]\hat{\boldsymbol g}_{b2}. \end{aligned} \tag{20}$$

Equation (20) describes the Green's function of the two-impurity problem and it has a form of the Dyson equation for the $\hat{\mathcal T}$ operator: $\hat{\boldsymbol G} = \hat{\boldsymbol g} + \hat{\boldsymbol g}\hat{\mathcal T}\hat{\boldsymbol g}$ [11]. In Eq. (20), $\hat{\boldsymbol g}_{1a}$, $\hat{\boldsymbol g}_{1b}$, and $\hat{\boldsymbol g}_{12}$ are scalars so below we omit the matrix signs. The operators $\hat{\boldsymbol Z}_a$, $\hat{\boldsymbol Z}_b$, $\hat{\boldsymbol T}^i$ with $i \in \{A, B, C, D\}$ are 2×2 matrices. The operators $\hat{\boldsymbol Z}_a$, $\hat{\boldsymbol Z}_b$ are given in Eq. (7). To determine $\hat{\boldsymbol T}^A, \hat{\boldsymbol T}^B, \hat{\boldsymbol T}^C, \hat{\boldsymbol T}^D$ we use the Woodbury identities.

B. Matrix inversion by Woodbury identities

Let $\hat{A}$, $\hat{B}$, $\hat{C}$, $\hat{D}$ be noncommuting operators in Eq. (17). Then, the Woodbury formula states [16]

$$\hat{T} = \hat{Y}^{-1} = \begin{bmatrix} +\hat{\Delta}_1^{-1} & -\hat{\Delta}_1^{-1}\hat{B}\hat{D}^{-1} \\ -\hat{\Delta}_2^{-1}\hat{C}\hat{A}^{-1} & +\hat{\Delta}_2^{-1} \end{bmatrix}, \tag{21}$$

where

$$\hat{\Delta}_1 = \hat{A} - \hat{B}\hat{D}^{-1}\hat{C}, \tag{22}$$

$$\hat{\Delta}_2 = \hat{D} - \hat{C}\hat{A}^{-1}\hat{B}. \tag{23}$$

Turning to Eq. (17) we note that in this case $\hat{A}$ commutes with $\hat{C}$, and $\hat{B}$ commutes with $\hat{D}$. This gives $\hat{\Delta}_1 = \hat{D}^{-1}\hat{F}_1$ and $\hat{\Delta}_2 = \hat{A}^{-1}\hat{F}_2$, where

$$\hat{F}_1 = \hat{D}\hat{A} - \hat{B}\hat{C}, \tag{24}$$

$$\hat{F}_2 = \hat{A}\hat{D} - \hat{C}\hat{B}, \tag{25}$$

respectively. Then, from Eq. (21) one has

$$\hat{T} = \begin{bmatrix} +\hat{F}_1^{-1}\hat{D} & -\hat{F}_1^{-1}\hat{B} \\ -\hat{F}_2^{-1}\hat{C} & +\hat{F}_2^{-1}\hat{A} \end{bmatrix}. \tag{26}$$

From Eqs. (16), (18), and (24)–(26) there is

$$\hat{T} = \begin{bmatrix} \hat{F}_1^{-1}(\hat{I} - g_0\hat{Z}_b) & \hat{F}_1^{-1}g_{ab}\hat{Z}_b, \\ \hat{F}_2^{-1}g_{ba}\hat{Z}_a & \hat{F}_2^{-1}(\hat{I} - g_0\hat{Z}_a) \end{bmatrix}, \tag{27}$$

where $g_{aa} = g_{bb} \equiv g_0$. We assume that g_0 is finite (see Sec. IX). From Eqs. (20) and (27) we have

$$\begin{aligned} \hat{G}_{12} = {} & g_{12}\hat{I} + g_{1a}[\hat{Z}_a\hat{F}_1^{-1}(\hat{I} - g_0\hat{Z}_b)]g_{a2} \\ & + g_{1a}[g_{ab}\hat{Z}_a\hat{F}_1^{-1}\hat{Z}_b]g_{b2} + g_{1b}[g_{ba}\hat{Z}_b\hat{F}_2^{-1}\hat{Z}_a]g_{a2} \\ & + g_{1b}[\hat{Z}_b\hat{F}_2^{-1}(\hat{I} - g_0\hat{Z}_a)]g_{b2}. \end{aligned} \tag{28}$$

Introducing operators $\hat{Q}_1 = \hat{F}_1^{-1}$ and $\hat{Q}_2 = \hat{F}_2^{-1}$ we rewrite Eq. (28) as

$$\begin{aligned} \hat{G}_{12} = {} & g_{12}\hat{I} + g_{1a}[\hat{Z}_a\hat{Q}_1(\hat{I} - g_0\hat{Z}_b)]g_{a2} \\ & + g_{1a}[g_{ab}\hat{Z}_a\hat{Q}_1\hat{Z}_b]g_{b2} + g_{1b}[g_{ba}\hat{Z}_b\hat{Q}_2\hat{Z}_a]g_{a2} \\ & + g_{1b}[\hat{Z}_b\hat{Q}_2(\hat{I} - g_0\hat{Z}_a)]g_{b2}. \end{aligned} \tag{29}$$

From Eqs. (16) and (24) and (25) we find

$$\hat{F}_1 = [(\hat{I} - g_0\hat{Z}_b)(\hat{I} - g_0\hat{Z}_a) - g_{ab}g_{ba}\hat{Z}_b\hat{Z}_a] = \hat{Q}_1^{-1}, \tag{30}$$

$$\hat{F}_2 = [(\hat{I} - g_0\hat{Z}_a)(\hat{I} - g_0\hat{Z}_b) - g_{ab}g_{ba}\hat{Z}_a\hat{Z}_b] = \hat{Q}_2^{-1}. \tag{31}$$

Equations (29)–(31) describe the exact GF of the considered system. The operators $\hat{Q}_1$ and $\hat{Q}_2$ are 2×2 matrices defined as the inversions of $\hat{F}_1$ and $\hat{F}_2$ matrices, which are combinations of $\hat{S}_a$ and $\hat{S}_b$ operators. In two limiting cases of small and large $|J|$, the operators $\hat{F}_1$ and $\hat{F}_2$ can be inverted explicitly. For arbitrary J we must invert $\hat{F}_1, \hat{F}_2$ using the general form of Woodbury identities in Eq. (21) (see below).

For small s-d coupling there is $g_0\hat{Z}_a \ll \hat{I}$, $g_0\hat{Z}_b \ll \hat{I}$, $g_{ab}g_{ba}\hat{Z}_b\hat{Z}_a \ll \hat{I}$, so one can disregard these terms. Then, one obtains in Eqs. (30) and (31) $\hat{F}_1 \simeq \hat{I}$, $\hat{F}_2 \simeq \hat{I}$, and, consequently, $\hat{Q}_1, \hat{Q}_2 \simeq \hat{I}$. Then, Eq. (29) reduces to

$$\begin{aligned} \hat{G}_{12} \simeq {} & \hat{g}_{12} + g_{1a}\hat{Z}_a g_{a2} + g_{1a}g_{ab}\hat{Z}_a\hat{Z}_b g_{b2} + g_{1b}g_{ba}\hat{Z}_b\hat{Z}_a g_{a2} \\ & + g_{1b}\hat{Z}_b g_{b2}. \end{aligned} \tag{32}$$

Equation (32) describes the first and second order terms of the Born series for two-point spin-dependent potential

$$\hat{G} \simeq \hat{g} + \hat{g}(V_a + V_b)\hat{g} + \hat{g}(V_a + V_b)\hat{g}(V_a + V_b)\hat{g} + \cdots . \tag{33}$$

Calculating the range function $\mathcal{J}(r_{ab})$ with use of GF in Eq. (32) one obtains the standard result for RKKY interaction (see Appendix B).

For the strong coupling there is $g_0\hat{Z}_a \gg \hat{I}$, $g_0\hat{Z}_b \gg \hat{I}$, and $g_{ab}g_{ba}\hat{Z}_b\hat{Z}_a \gg \hat{I}$, so that one can disregard the identity operator $\hat{I}$ in Eqs. (30) and (31). Then, the expressions in Eqs. (30) and (31) reduce to products of two operators, that can be inverted in the standard way. The GF in Eq. (29) and the range function in this limit are obtained and discussed in Appendix C.

IV. EXACT GREEN'S FUNCTION FOR ARBITRARY SPINS

Let $\hat{F}_1 = \begin{bmatrix} \hat{f}^{1A} & \hat{f}^{1B} \\ \hat{f}^{1C} & \hat{f}^{1D} \end{bmatrix}$, in which

$$\hat{f}^{1A} = p_2\left(\hat{S}_b^-\hat{S}_a^+ + \hat{S}_b^z\hat{S}_a^z\right) - p_1\left(\hat{S}_b^z + \hat{S}_a^z\right) + 1, \tag{34}$$

$$\hat{f}^{1B} = p_2\left(\hat{S}_b^z\hat{S}_a^- - \hat{S}_b^-\hat{S}_a^z\right) - p_1(\hat{S}_b^- + \hat{S}_a^-), \tag{35}$$

$$\hat{f}^{1C} = p_2\left(\hat{S}_b^+\hat{S}_a^z - \hat{S}_b^z\hat{S}_a^+\right) - p_1(\hat{S}_b^+ + \hat{S}_a^+), \tag{36}$$

$$\hat{f}^{1D} = p_2\left(\hat{S}_b^+\hat{S}_a^- + \hat{S}_b^z\hat{S}_a^z\right) + p_1\left(\hat{S}_b^z + \hat{S}_a^z\right) + 1, \tag{37}$$

and

$$p_1 = \tfrac{1}{2}Jg_0, \tag{38}$$

$$p_2 = \tfrac{1}{4}J^2\left(g_0^2 - g_{ab}g_{ba}\right) \equiv J^2 p_2^{ab}. \tag{39}$$

To obtain $\hat{F}_2$ one should exchange a and b indices in Eqs. (34)–(37). Let

$$\hat{Q}_1 \equiv \hat{F}_1^{-1} = \begin{bmatrix} \hat{q}^{1A} & \hat{q}^{1B} \\ \hat{q}^{1C} & \hat{q}^{1D} \end{bmatrix}. \tag{40}$$

Using Eq. (21) we find

$$\hat{Q}_1 = \begin{bmatrix} \hat{\Delta}_{1A}^{-1} & -\hat{\Delta}_{1A}^{-1}\hat{f}^{1B}(\hat{f}^{1D})^{-1} \\ -\hat{\Delta}_{1D}^{-1}\hat{f}^{1C}(\hat{f}^{1A})^{-1} & \hat{\Delta}_{1D}^{-1} \end{bmatrix}, \tag{41}$$

in which

$$\hat{\Delta}_{1A} = \hat{f}^{1A} - \hat{f}^{1B}(\hat{f}^{1D})^{-1}\hat{f}^{1C}, \tag{42}$$

$$\hat{\Delta}_{1D} = \hat{f}^{1D} - \hat{f}^{1C}(\hat{f}^{1A})^{-1}\hat{f}^{1B}. \tag{43}$$

Similarly, let

$$\hat{Q}_2 \equiv \hat{F}_2^{-1} = \begin{bmatrix} \hat{q}^{2A} & \hat{q}^{2B} \\ \hat{q}^{2C} & \hat{q}^{2D} \end{bmatrix}. \tag{44}$$

Using Eq. (21) we find

$$\hat{Q}_2 = \begin{bmatrix} \hat{\Delta}_{2A}^{-1} & -\hat{\Delta}_{2A}^{-1}\hat{f}^{2B}(\hat{f}^{2D})^{-1} \\ -\hat{\Delta}_{2D}^{-1}\hat{f}^{2C}(\hat{f}^{2A})^{-1} & \hat{\Delta}_{2D}^{-1} \end{bmatrix}, \tag{45}$$

in which

$$\hat{\Delta}_{2A} = \hat{f}^{2A} - \hat{f}^{2B}(\hat{f}^{2D})^{-1}\hat{f}^{2C}, \tag{46}$$

$$\hat{\Delta}_{2D} = \hat{f}^{2D} - \hat{f}^{2C}(\hat{f}^{2A})^{-1}\hat{f}^{2B}. \tag{47}$$

Then, one obtains from Eqs. (29), (40), and (44)

$$\hat{\boldsymbol{G}} = \hat{\boldsymbol{G}}^{aa} + \hat{\boldsymbol{G}}^{ab} + \hat{\boldsymbol{G}}^{ba} + \hat{\boldsymbol{G}}^{bb}, \tag{48}$$

which can be rewritten as a 2 × 2 matrix equation

$$\begin{pmatrix} (\hat{G})_{11} & (\hat{G})_{12} \\ (\hat{G})_{21} & (\hat{G})_{22} \end{pmatrix} = \begin{pmatrix} (\hat{G}^{aa})_{11} & (\hat{G}^{aa})_{12} \\ (\hat{G}^{aa})_{21} & (\hat{G}^{aa})_{22} \end{pmatrix} + \begin{pmatrix} (\hat{G}^{ab})_{11} & (\hat{G}^{ab})_{12} \\ (\hat{G}^{ab})_{21} & (\hat{G}^{ab})_{22} \end{pmatrix} + \begin{pmatrix} (\hat{G}^{ba})_{11} & (\hat{G}^{ba})_{12} \\ (\hat{G}^{ba})_{21} & (\hat{G}^{ba})_{22} \end{pmatrix} + \begin{pmatrix} (\hat{G}^{bb})_{11} & (\hat{G}^{bb})_{12} \\ (\hat{G}^{bb})_{21} & (\hat{G}^{bb})_{22} \end{pmatrix}, \tag{49}$$

where

$$(\hat{G}^{aa})_{11} = g_{1a}\left\{-\frac{J^2}{4}g_0\left(\hat{S}_a^-\hat{q}^{1C}\hat{S}_b^z - \hat{S}_a^-\hat{q}^{1D}\hat{S}_b^+ - \hat{S}_a^z\hat{q}^{1A}\hat{S}_b^z - \hat{S}_a^z\hat{q}^{1B}\hat{S}_b^+\right) + \frac{J}{2}\left(\hat{S}_a^-\hat{q}^{1C} + \hat{S}_a^z\hat{q}^{1A}\right)\right\}g_{a2}, \tag{50}$$

$$(\hat{G}^{aa})_{12} = g_{1a}\left\{-\frac{J^2}{4}g_0\left(\hat{S}_a^-\hat{q}^{1C}\hat{S}_b^- + \hat{S}_a^-\hat{q}^{1D}\hat{S}_b^z - \hat{S}_a^z\hat{q}^{1A}\hat{S}_b^- + \hat{S}_a^z\hat{q}^{1B}\hat{S}_b^z\right) + \frac{J}{2}\left(\hat{S}_a^-\hat{q}^{1D} + \hat{S}_a^z\hat{q}^{1B}\right)\right\}g_{a2}, \tag{51}$$

$$(\hat{G}^{aa})_{21} = g_{1a}\left\{-\frac{J^2}{4}g_0\left(\hat{S}_a^+\hat{q}^{1A}\hat{S}_b^z - \hat{S}_a^+\hat{q}^{1B}\hat{S}_b^+ + \hat{S}_a^z\hat{q}^{1C}\hat{S}_b^z + \hat{S}_a^z\hat{q}^{1D}\hat{S}_b^+\right) + \frac{J}{2}\left(\hat{S}_a^+\hat{q}^{1A} - \hat{S}_a^z\hat{q}^{1C}\right)\right\}g_{a2}, \tag{52}$$

$$(\hat{G}^{aa})_{22} = g_{1a}\left\{-\frac{J^2}{4}g_0\left(\hat{S}_a^+\hat{q}^{1A}\hat{S}_b^- + \hat{S}_a^+\hat{q}^{1B}\hat{S}_b^z + \hat{S}_a^z\hat{q}^{1C}\hat{S}_b^- - \hat{S}_a^z\hat{q}^{1D}\hat{S}_b^z\right) + \frac{J}{2}\left(\hat{S}_a^+\hat{q}^{1B} - \hat{S}_a^z\hat{q}^{1D}\right)\right\}g_{a2}, \tag{53}$$

$$(\hat{G}^{ab})_{11} = g_{1a}\left\{\frac{J^2}{4}g_{ab}\left(\hat{S}_a^-\hat{q}^{1C}\hat{S}_b^z + \hat{S}_a^-\hat{q}^{1D}\hat{S}_b^+ + \hat{S}_a^z\hat{q}^{1A}\hat{S}_b^z + \hat{S}_a^z\hat{q}^{1B}\hat{S}_b^+\right)\right\}g_{b2}, \tag{54}$$

$$(\hat{G}^{ab})_{12} = g_{1a}\left\{\frac{J^2}{4}g_{ab}\left(\hat{S}_a^-\hat{q}^{1C}\hat{S}_b^- - \hat{S}_a^-\hat{q}^{1D}\hat{S}_b^z + \hat{S}_a^z\hat{q}^{1A}\hat{S}_b^- - \hat{S}_a^z\hat{q}^{1B}\hat{S}_b^z\right)\right\}g_{b2}, \tag{55}$$

$$(\hat{G}^{ab})_{21} = g_{1a}\left\{\frac{J^2}{4}g_{ab}\left(\hat{S}_a^+\hat{q}^{1A}\hat{S}_b^z + \hat{S}_a^+\hat{q}^{1B}\hat{S}_b^+ - \hat{S}_a^z\hat{q}^{1C}\hat{S}_b^z - \hat{S}_a^z\hat{q}^{1D}\hat{S}_b^+\right)\right\}g_{b2}, \tag{56}$$

$$(\hat{G}^{ab})_{22} = g_{1a}\left\{\frac{J^2}{4}g_{ab}\left(\hat{S}_a^+\hat{q}^{1A}\hat{S}_b^- - \hat{S}_a^+\hat{q}^{1B}\hat{S}_b^z - \hat{S}_a^z\hat{q}^{1C}\hat{S}_b^- + \hat{S}_a^z\hat{q}^{1D}\hat{S}_b^z\right)\right\}g_{b2}, \tag{57}$$

$$(\hat{G}^{ba})_{11} = g_{1b}\left\{\frac{J^2}{4}g_{ba}\left(\hat{S}_b^-\hat{q}^{2C}\hat{S}_a^z + \hat{S}_b^-\hat{q}^{2D}\hat{S}_a^+ + \hat{S}_b^z\hat{q}^{2A}\hat{S}_a^z + \hat{S}_b^z\hat{q}^{2B}\hat{S}_a^+\right)\right\}g_{a2}, \tag{58}$$

$$(\hat{G}^{ba})_{12} = g_{1b}\left\{\frac{J^2}{4}g_{ba}\left(\hat{S}_b^-\hat{q}^{2C}\hat{S}_a^- - \hat{S}_b^-\hat{q}^{2D}\hat{S}_a^z + \hat{S}_b^z\hat{q}^{2A}\hat{S}_a^- - \hat{S}_b^z\hat{q}^{2B}\hat{S}_a^z\right)\right\}g_{a2}, \tag{59}$$

$$(\hat{G}^{ba})_{21} = g_{1b}\left\{\frac{J^2}{4}g_{ba}\left(\hat{S}_b^+\hat{q}^{2A}\hat{S}_a^z + \hat{S}_b^+\hat{q}^{2B}\hat{S}_a^+ - \hat{S}_b^z\hat{q}^{2C}\hat{S}_a^z - \hat{S}_b^z\hat{q}^{2D}\hat{S}_a^+\right)\right\}g_{a2}, \tag{60}$$

$$(\hat{G}^{ba})_{22} = g_{1b}\left\{\frac{J^2}{4}g_{ba}\left(\hat{S}_b^+\hat{q}^{2A}\hat{S}_a^- - \hat{S}_b^+\hat{q}^{2B}\hat{S}_a^z - \hat{S}_b^z\hat{q}^{2C}\hat{S}_a^- + \hat{S}_b^z\hat{q}^{2D}\hat{S}_a^z\right)\right\}g_{a2}, \tag{61}$$

$$(\hat{G}^{bb})_{11} = g_{1b}\left\{-\frac{J^2}{4}g_0\left(\hat{S}_b^-\hat{q}^{2C}\hat{S}_a^z - \hat{S}_b^-\hat{q}^{2D}\hat{S}_a^+ - \hat{S}_b^z\hat{q}^{2A}\hat{S}_a^z - \hat{S}_b^z\hat{q}^{2B}\hat{S}_a^+\right) + \frac{J}{2}\left(\hat{S}_b^-\hat{q}^{2C} + \hat{S}_b^z\hat{q}^{2A}\right)\right\}g_{b2}, \tag{62}$$

$$(\hat{G}^{bb})_{12} = g_{1b}\left\{-\frac{J^2}{4}g_0\left(\hat{S}_b^-\hat{q}^{2C}\hat{S}_a^- + \hat{S}_b^-\hat{q}^{2D}\hat{S}_a^z - \hat{S}_b^z\hat{q}^{2A}\hat{S}_a^- + \hat{S}_b^z\hat{q}^{2B}\hat{S}_a^z\right) + \frac{J}{2}\left(\hat{S}_b^-\hat{q}^{2D} + \hat{S}_b^z\hat{q}^{2B}\right)\right\}g_{b2}, \tag{63}$$

$$(\hat{G}^{bb})_{21} = g_{1b}\left\{-\frac{J^2}{4}g_0\left(\hat{S}_b^+\hat{q}^{2A}\hat{S}_a^z - \hat{S}_b^+\hat{q}^{2B}\hat{S}_a^+ + \hat{S}_b^z\hat{q}^{2C}\hat{S}_a^z + \hat{S}_b^z\hat{q}^{2D}\hat{S}_a^+\right) + \frac{J}{2}\left(\hat{S}_b^+\hat{q}^{2A} - \hat{S}_b^z\hat{q}^{2C}\right)\right\}g_{b2}, \tag{64}$$

$$(\hat{G}^{bb})_{22} = g_{1b}\left\{-\frac{J^2}{4}g_0\left(\hat{S}_b^+\hat{q}^{2A}\hat{S}_a^- + \hat{S}_b^+\hat{q}^{2B}\hat{S}_a^z + \hat{S}_b^z\hat{q}^{2C}\hat{S}_a^- - \hat{S}_b^z\hat{q}^{2D}\hat{S}_a^z\right) + \frac{J}{2}\left(\hat{S}_b^+\hat{q}^{2B} - \hat{S}_b^z\hat{q}^{2D}\right)\right\}g_{b2}. \tag{65}$$

Equations (49)–(65) describe the exact GF of electron gas in the presence of two pointlike impurities with arbitrary spins $\hat{S}_a$ and $\hat{S}_b$. The operators $\hat{q}^{1\alpha}, \hat{q}^{2\alpha}$ with $\alpha = A, B, C, D$ are defined in Eqs. (40) and (44), respectively. The terms $\hat{G}^{ab}$ and $\hat{G}^{ba}$ correspond, roughly, to interactions between spins, while $\hat{G}^{aa}$ and $\hat{G}^{bb}$ describe one-site properties. By taking the limit $Jg_0 \to 0$ in Eqs. (34)–(39) (corresponding to $p_1, p_2 \to 0$) we find $\hat{f}^{1A}, \hat{f}^{2A}, \hat{f}^{1D}, \hat{f}^{2D} \simeq 1$, while the remaining terms vanish. There is also $\hat{q}^{1A}, \hat{q}^{1D}, \hat{q}^{2A}, \hat{q}^{2D} \simeq 1$, and the remaining terms vanish. Assuming $g_{ab} = g_{ba}$ one obtains for the electron density $n(E)$

$$n(E) = -\frac{1}{\pi}\mathrm{Im}\mathrm{Tr}(\hat{\boldsymbol{G}}) = -\frac{J^2}{\pi}\left(\mathrm{Im}\int g_{1a}g_{b1}g_{ab}d^3\boldsymbol{r}\right)\hat{\boldsymbol{S}}_a\hat{\boldsymbol{S}}_b, \tag{66}$$

which is the density of states obtained for the RKKY interaction (see Appendix B). In Eqs. (50)–(65) there is no symmetry between positive and negative values of the coupling constant J because of the linear terms in J. The expressions in curly brackets in Eqs. (50)–(65) are the matrix elements of the $\hat{\mathcal{T}}$ operator.

For arbitrary spins $\hat{S}_a, \hat{S}_b$ one can not find general expressions for $\hat{\boldsymbol{G}}$ in a closed form because the operators $\hat{q}^{1\alpha}, \hat{q}^{2\alpha}$ with $\alpha = A, B, C, D$ in Eqs. (49)–(65) are nonlinear functions of $\hat{S}_a, \hat{S}_b$ [see Eqs. (40)–(47)]. However, it is possible to obtain matrix elements of $\hat{\boldsymbol{G}}$ using a method described in the next section. Additionally, for $\hat{S}_a, \hat{S}_b = \frac{1}{2}$ it is possible to find analytical expressions for $\hat{q}^{1\alpha}$ and $\hat{q}^{2\alpha}$. This allows one to express the exact GF in Eqs. (49)–(65) as a bilinear combination of $\hat{S}_a, \hat{S}_b$ components.

V. MATRIX ELEMENTS OF GF COMPONENTS

Here, we present a general method of calculation of the matrix elements of $\hat{\boldsymbol{G}}$ components, as given in Eqs. (49)–(65). This method may be applied for arbitrary spin values $\hat{S}_a, \hat{S}_b = \frac{1}{2}, 1, \frac{3}{2}, \dots$ and we illustrate it for $\hat{S}_a, \hat{S}_b = \frac{1}{2}$.

Consider the Zeeman basis $\mathcal{B}_{1/2}$ for spins $\hat{S}_a, \hat{S}_b = \frac{1}{2}$ in which each state $|n\rangle$ is labeled by two zth components the spins $|n\rangle = |S_a^z, S_b^z\rangle$. The basis $\mathcal{B}_{1/2}$ consists of four vectors

$$\begin{aligned}\mathcal{B}_{1/2} &= \{|\uparrow,\uparrow\rangle, |\uparrow,\downarrow\rangle, |\downarrow,\uparrow\rangle, |\downarrow,\downarrow\rangle\} \\ &\equiv \{|1\rangle, |2\rangle, 3\rangle, |4\rangle\},\end{aligned} \tag{67}$$

where the up and down arrows indicate states with $S_z = +\frac{1}{2}$ and $S_z = -\frac{1}{2}$, respectively. For arbitrary spins such a basis consists of $(2S_a + 1)(2S_b + 1)$ elements. In the basis $\mathcal{B}_{1/2}$ the spin operators $\hat{S}_a^{\pm}, \hat{S}_b^{\pm}, \hat{S}_a^z, \hat{S}_b^z$ are 4×4 matrices

$$\hat{S}_a^+ = \begin{pmatrix} 0 & 0 & 1 & 0 \\ 0 & 0 & 0 & 1 \\ 0 & 0 & 0 & 0 \\ 0 & 0 & 0 & 0 \end{pmatrix}, \tag{68}$$

$$\hat{S}_b^+ = \begin{pmatrix} 0 & 1 & 0 & 0 \\ 0 & 0 & 0 & 0 \\ 0 & 0 & 0 & 1 \\ 0 & 0 & 0 & 0 \end{pmatrix}, \tag{69}$$

and $\hat{S}_a^- = (\hat{S}_a^+)^\dagger$, $\hat{S}_b^- = (\hat{S}_b^+)^\dagger$. There is also $\hat{S}_a^z = \mathrm{diag}(\frac{1}{2}, \frac{1}{2}, -\frac{1}{2}, -\frac{1}{2})$ and $\hat{S}_b^z = \mathrm{diag}(\frac{1}{2}, -\frac{1}{2}, \frac{1}{2}, -\frac{1}{2})$, where "diag" represents the diagonal matrix. In this representation, each state $|n\rangle$ with $n = 1, \dots, 4$ is a four-component column vector with the nth element equal to unity and remaining elements equal to zero. In the basis $\mathcal{B}_{1/2}$ the operators $\hat{f}_{1\alpha}, \hat{f}_{2\alpha}$ with $\alpha = A, B, C, D$ in Eqs. (34)–(37) are 4×4 matrices [see Eqs. (S137)–(S140) in the Supplemental Material [7]]. Calculating appropriate products, sums and inverses of these matrices [see Eqs. (S145)–(S152) and (S153)–(S192) in the Supplemental Material [7]], one obtains the 4×4 matrices describing the $\hat{q}^{1\alpha}, \hat{q}^{2\alpha}$ operators. Inserting these matrices into Eqs. (49)–(65) one obtains $\hat{\boldsymbol{G}}$, which is also a 4×4 matrix in the representation $\mathcal{B}_{1/2}$. To find the matrix element of $\hat{\boldsymbol{G}}$ between two states $|n\rangle$ and $|n'\rangle$, with $n, n' = 1, \dots, 4$ one multiplies $\hat{\boldsymbol{G}}$ by two appropriate four-element vectors.

As an example of the above procedure we consider the third term of Eq. (50),

$$(\hat{G}^{ab})_{11|3} = \tfrac{1}{4} g_{1a} g_{ab} g_{b2} J^2 \hat{S}_a^z \hat{q}^{1A} \hat{S}_b^z \equiv C_3 \hat{S}_a^z \hat{q}^{1A} \hat{S}_b^z, \tag{70}$$

where $C_3 = (J^2/4) g_{1a} g_{ab} g_{b2}$ is a c number. Using Eqs. (S145)–(S152) in the Supplemental Material [7] there is

$$(\hat{G}^{ab})_{11|3} = C_3 \begin{pmatrix} \frac{1}{2} & 0 & 0 & 0 \\ 0 & \frac{1}{2} & 0 & 0 \\ 0 & 0 & -\frac{1}{2} & 0 \\ 0 & 0 & 0 & -\frac{1}{2} \end{pmatrix} \begin{pmatrix} q_{11}^{1A} & 0 & 0 & 0 \\ 0 & q_{22}^{1A} & q_{23}^{1A} & 0 \\ 0 & q_{32}^{1A} & q_{33}^{1A} & 0 \\ 0 & 0 & 0 & q_{44}^{1A} \end{pmatrix} \begin{pmatrix} \frac{1}{2} & 0 & 0 & 0 \\ 0 & -\frac{1}{2} & 0 & 0 \\ 0 & 0 & \frac{1}{2} & 0 \\ 0 & 0 & 0 & -\frac{1}{2} \end{pmatrix} = \frac{C_3}{4} \begin{pmatrix} q_{11}^{1A} & 0 & 0 & 0 \\ 0 & -q_{22}^{1A} & q_{23}^{1A} & 0 \\ 0 & q_{32}^{1A} & -q_{33}^{1A} & 0 \\ 0 & 0 & 0 & q_{44}^{1A} \end{pmatrix}, \tag{71}$$

where $q_{22}^{1A}, q_{23}^{1A}, q_{32}^{1A}, q_{33}^{1A}, q_{44}^{1A}$ are c numbers [see Eqs. (S153)–(S192) in Supplemental Material [7]]. The matrix element of $(\hat{G}^{ab})_{11|3}$ between two states $|1\rangle$ is then $C_3 q_{11}^{1A}/4$.

The procedure described above is convenient for calculation of the matrix elements of $\hat{\boldsymbol{G}}$ for arbitrary spins. Since the largest value of spin in stable isotopes is $S = 5$, corresponding to ^{138}La [17], the largest number of basis states is $(2S + 1)^2 = 121$.

In the general case, the matrix form of $\hat{S}_c^+, \hat{S}_c^-, \hat{S}_c^z$ operators ($c = a, b$) can be obtained with use of standard formulas

$$\langle S, m' | \hat{S}^z | S, m\rangle = m\delta_{m'm}, \tag{72}$$

$$\langle S, m' | \hat{S}^+ | S, m\rangle = \delta_{m'm+1}\sqrt{S(S-1) - m'm}, \tag{73}$$

$$\langle S, m' | \hat{S}^- | S, m\rangle = \delta_{m+1'm}\sqrt{S(S-1) - m'm}, \tag{74}$$

where S is an arbitrary spin whose S_z components are labeled by $m = -S, -S+1, \dots, S$. Using the above identities one can construct operators $\hat{S}_a^{\pm}$, $\hat{S}_b^{\pm}$, $\hat{S}_a^z$, $\hat{S}_b^z$ analogous to those in Eqs. (68) and (69), which are now $(2S_a + 1)(2S_b + 1) \times (2S_a + 1)(2S_b + 1)$ matrices. Then, the matrix elements of exact GF are obtained in the same way as those for $\hat{S}_a, \hat{S}_b = \frac{1}{2}$ spins.

All numerical results obtained in Figs. 1–3 and Tables II and III in Section X can be derived using the method described above. We checked that they agree with results obtained using expressions in Sec. VII. However, despite the fact that the described method is suitable for numerical calculation, it gives little understanding of the physical nature of exact GF and its dependence on the four physical parameters: m^*, J, r_{ab}, and E_F. For this reason, for the special case $\hat{S}_a, \hat{S}_b = \frac{1}{2}$ we reexpress exact GF in terms of components of spin operators, which allows us to reduce the range function $\mathcal{J}(r_{ab})$ to integrals of analytical expressions.

VI. SPIN-OPERATOR FORM OF GF COMPONENTS

Here, we express the operators $\hat{G}_{11}$, $\hat{G}_{12}$, $\hat{G}_{21}$, $\hat{G}_{22}$ in Eqs. (49)–(65) as linear combinations of spin operators $\hat{S}_a^{\pm}$, $\hat{S}_b^{\pm}$ and $\hat{S}_a^z$, $\hat{S}_b^z$. This form of exact GF is more convenient for analysis the range function properties.

In the representation of Eq. (67), both components of $\hat{S}_a$, $\hat{S}_b$ spins and matrices $\hat{q}^{1\alpha}$, $\hat{q}^{2\alpha}$ have at most 14 nonzero elements. For all these matrices the elements (1,4) and (4,1) vanish. Then, each term on the right-hand side of Eqs. (50)–(65) can be expressed as a linear combination of 14 linearly independent 4×4 matrices $\hat{\Lambda}^{mn}$ having only one nonzero element (m, n) except elements (1,4) and (4,1) which are always zero. In the next step, one expresses the matrices $\hat{\Lambda}^{mn}$ as combinations of operators $\hat{S}_a^{\pm}$, $\hat{S}_b^{\pm}$, $\hat{S}_a^z$, $\hat{S}_b^z$ and their products [see Eqs. (68) and (69)]. Then, one obtains

$$\hat{\Lambda}^{11} = \hat{I}/4 + \hat{S}_a^z/2 + \hat{S}_b^z/2 + \hat{S}_a^z\hat{S}_b^z, \tag{75}$$

$$\hat{\Lambda}^{12} = \hat{S}_b^+(\hat{I}/2 + \hat{S}_a^z), \tag{76}$$

$$\hat{\Lambda}^{13} = \hat{S}_a^+(\hat{I}/2 + \hat{S}_b^z), \tag{77}$$

$$\hat{\Lambda}^{21} = \hat{S}_b^-(\hat{I}/2 + \hat{S}_a^z), \tag{78}$$

$$\hat{\Lambda}^{22} = \hat{I}/4 + \hat{S}_a^z/2 - \hat{S}_b^z/2 - \hat{S}_a^z\hat{S}_b^z, \tag{79}$$

$$\hat{\Lambda}^{23} = \hat{S}_a^+\hat{S}_b^-, \tag{80}$$

$$\hat{\Lambda}^{24} = \hat{S}_a^+(\hat{I}/2 - \hat{S}_b^z), \tag{81}$$

$$\hat{\Lambda}^{31} = \hat{S}_a^-(\hat{I}/2 + \hat{S}_b^z), \tag{82}$$

$$\hat{\Lambda}^{32} = \hat{S}_a^-\hat{S}_b^+, \tag{83}$$

$$\hat{\Lambda}^{33} = \hat{I}/4 - \hat{S}_a^z/2 + \hat{S}_b^z/2 - \hat{S}_a^z\hat{S}_b^z, \tag{84}$$

$$\hat{\Lambda}^{34} = \hat{S}_b^+(\hat{I}/2 - \hat{S}_a^z), \tag{85}$$

$$\hat{\Lambda}^{42} = \hat{S}_a^-(\hat{I}/2 - \hat{S}_b^z), \tag{86}$$

$$\hat{\Lambda}^{43} = \hat{S}_b^-(\hat{I}/2 - \hat{S}_a^z), \tag{87}$$

$$\hat{\Lambda}^{44} = \hat{I}/4 - \hat{S}_a^z/2 - \hat{S}_b^z/2 + \hat{S}_a^z\hat{S}_b^z, \tag{88}$$

where $\hat{I}$ is the 4×4 identity matrix and $\hat{\Lambda}^{14}, \hat{\Lambda}^{41} = 0$. Having defined operators $\hat{\Lambda}^{mn}$ one can expand the functions $\hat{G}_{ij}^{\alpha\beta}$ in Eqs. (50)–(65), with $c, d = a, b$ and $i, j = 1, 2$ in linear combinations of $\hat{\Lambda}^{mn}$ operators. Finally, using Eqs. (75)–(88), one expresses each term on the right-hand side of Eqs. (50)–(65) as a linear combination of products of components of $\hat{S}_a$, $\hat{S}_b$ operators. The formulas are shown in Eqs. (S1)–(S124) in the Supplemental Material [7]. These equations represent the exact GF of a free-electron gas interacting with two localized spin moments $\hat{S} = \frac{1}{2}$. They are bilinear combinations of spin operators $\{\hat{S}_a^+, \hat{S}_a^-, \hat{S}_a^z, \hat{S}_b^+, \hat{S}_b^-, \hat{S}_b^z\}$. In contrast, the expressions in Eqs. (50)–(65) are nonlinear combinations of spin operators because of the presence of $\hat{q}^{1\alpha}$, $\hat{q}^{2\alpha}$ operators.

Analytical expressions for elements of $\hat{q}^{1\alpha}$, $\hat{q}^{2\alpha}$ matrices are shown in Eqs. (S153)–(S192) in the Supplemental Material [7]. The elements of these matrices, denoted as $q_{ij}^{1\alpha}$ and $q_{ij}^{2\alpha}$, are complex numbers depending on p_1 and p_2 only [see Eqs. (38) and (39)]. Both p_1 and p_2 depend on the value of the one-electron GF at the origin g_0, which we assumed to be finite and nonzero [see Eq. (10)].

To continue the example from Eqs. (70) we apply the above procedure to $(\hat{G}^{ab})_{11|3}$ in Eq. (71) and obtain

$$(\hat{G}^{ab})_{11|3} = \frac{C_3}{4}\big[\hat{\Lambda}^{11}q_{11}^{1A} - \hat{\Lambda}^{22}q_{22}^{1A} - \hat{\Lambda}^{33}q_{33}^{1A} + \hat{\Lambda}^{44}q_{44}^{1A} + \hat{\Lambda}^{23}q_{23}^{1A} + \hat{\Lambda}^{32}q_{32}^{1A}\big]. \tag{89}$$

Taking explicit forms of operators $\hat{\Lambda}^{11}$, $\hat{\Lambda}^{22}$, $\hat{\Lambda}^{23}$, $\hat{\Lambda}^{32}$, $\hat{\Lambda}^{33}$, $\hat{\Lambda}^{44}$ [see Eqs. (75)–(88)], one finds

$$\begin{aligned}(\hat{G}^{ab})_{11|3} = {} & \frac{C_3}{4}\left(\frac{1}{4}\hat{I} + \frac{1}{2}\hat{S}_a^z + \frac{1}{2}\hat{S}_b^z + \hat{S}_a^z\hat{S}_b^z\right)q_{11}^{1A} \\ & - \frac{C_3}{4}\left(\frac{1}{4}\hat{I} + \frac{1}{2}\hat{S}_a^z - \frac{1}{2}\hat{S}_b^z - \hat{S}_a^z\hat{S}_b^z\right)q_{22}^{1A} \\ & - \frac{C_3}{4}\left(\frac{1}{4}\hat{I} - \frac{1}{2}\hat{S}_a^z + \frac{1}{2}\hat{S}_b^z - \hat{S}_a^z\hat{S}_b^z\right)q_{33}^{1A} \\ & + \frac{C_3}{4}\left(\frac{1}{4}\hat{I} - \frac{1}{2}\hat{S}_a^z - \frac{1}{2}\hat{S}_b^z + \hat{S}_a^z\hat{S}_b^z\right)q_{44}^{1A} \\ & + \frac{C_3}{4}\hat{S}_a^+\hat{S}_b^-q_{23}^{1A} + \frac{C_3}{4}\hat{S}_a^-\hat{S}_b^+q_{32}^{1A}.\end{aligned} \tag{90}$$

In Eq. (90), the quantity $G_{11|3}^{ab}$ is a combination of products of localized spin components. The remaining terms of the exact GF are calculated in analogous way, and they are shown in Eqs. (S1)–(S124) in the Supplemental Material [7].

VII. GRAND CANONICAL POTENTIAL AND RANGE FUNCTIONS

Having obtained the exact GF one can calculate observables measured experimentally. We calculate the density of states (DOS), the grand canonical potential, the range function, and the energy of localized states. All calculations are performed for $T = 0$ but they can be generalized to nonzero temperatures using standard GF techniques (see Discussion, Sec. XI).

A. DOS and grand canonical potential

The continuous energy spectrum of the system is determined by the discontinuity of the Green's function along the cut of positive energy axis [18]. Then, the electron DOS is

$$n(E) = -\frac{1}{\pi}\mathrm{Im}\int \mathrm{Tr}\{\hat{\boldsymbol{G}}_{11}^+\}d^3\boldsymbol{r}, \tag{91}$$

where $\hat{\boldsymbol{G}}^+_{11} = \hat{\boldsymbol{G}}^+(\boldsymbol{r}_1, \boldsymbol{r}_1)$ and

$$\begin{aligned}\mathrm{Tr}\{\hat{\boldsymbol{G}}^+_{11}\} = {} & (\hat{\boldsymbol{G}}^{aa+})_{11} + (\hat{\boldsymbol{G}}^{aa+})_{22} + (\hat{\boldsymbol{G}}^{ab+})_{11} + (\hat{\boldsymbol{G}}^{ab+})_{22} \\ & + (\hat{\boldsymbol{G}}^{ba+})_{11} + (\hat{\boldsymbol{G}}^{ba+})_{22} + (\hat{\boldsymbol{G}}^{bb+})_{11} + (\hat{\boldsymbol{G}}^{bb+})_{22}.\end{aligned} \tag{92}$$

Calculating the trace in Eq. (91) from Eqs. (50)–(65) or Eqs. (S1)–(S124) in the Supplemental Material [7] we note that $\hat{\boldsymbol{G}}$ depends on spatial variables $\boldsymbol{r}_1$ and $\boldsymbol{r}_2$ by four products of one electron GFs, namely, $g_{1a}g_{a2}, g_{1a}g_{b2}, g_{1b}g_{a2}, g_{1b}g_{b2}$, while the remaining terms do not depend on $\boldsymbol{r}_1$ or $\boldsymbol{r}_2$. Taking the trace, one obtains three integrals

$$h^+_{ab} = h^+_{ba} = \int g^+_{1a}g^+_{b1}d^D\boldsymbol{r}_1 = -\frac{\partial g^+_{ab}}{\partial E}, \tag{93}$$

$$h^+_0 = \int g^+_{1a}g^+_{a1}d^D\boldsymbol{r}_1 = \lim_{b\to a} h^+_{ab}, \tag{94}$$

where $D = 1, 2, 3$ is system's dimensionality, and $g^+_{ab} = g^+_{ba}$. In Eqs. (93) and (94) we assumed the translational symmetry of the one-electron GF. To calculate quantities g^+_{ab}, h^+_{ab}, and h^+_0 one needs to specify the one-electron GF. We address this point in Sec. IX.

B. Range function

For noninteracting particles the generalized grand canonical potential is

$$\hat{\Omega} = -\int f(E)N(E)dE + \mu N, \tag{95}$$

ant it satisfies the proper extremal properties of the total energy [20]. Here, μ is the chemical potential, N is the number of particles, $f(E)$ is the Fermi-Dirac distribution function, and $N(E)$ is the integrated density of states

$$N(E) = \int_{-\infty}^{E} n(E')dE'. \tag{96}$$

Our calculations are limited to $T = 0$, and below we approximate $f(E) = \Theta(E_F - E)$, where $\Theta(x)$ is the step function and E_F is the Fermi energy.

In Eq. (95) the grand canonical potential $\hat{\Omega}$ depends on a configuration of spins $\hat{S}_a$ and $\hat{S}_b$. For $\hat{S}_a, \hat{S}_b = \frac{1}{2}$ one defines the range function $\mathcal{J}(r_{ab})$ as a difference between $\hat{\Omega}$ for parallel and antiparallel configurations of $\hat{S}_a$ and $\hat{S}_b$ spins

$$\mathcal{J}(r_{ab}) = \Omega_{\uparrow\uparrow} + \Omega_{\downarrow\downarrow} - (\Omega_{\uparrow\downarrow} + \Omega_{\downarrow\uparrow}), \tag{97}$$

where

$$\Omega_{\mu,\nu} = \langle \mu, \nu|\hat{\Omega}|\mu, \nu\rangle \tag{98}$$

is the grand canonical potential for a given configuration $\mu, \nu \in \{\uparrow, \downarrow\}$ of $\hat{S}_a$ and $\hat{S}_b$. Then, one can calculate $\mathcal{J}(r_{ab})$ numerically with the use of Eqs. (50)–(65).

The range function $\mathcal{J}(r_{ab})$ in Eq. (97) can be conveniently calculated for representation of GF given in Eqs. (S1)–(S124) in the Supplemental Material [7]. The derivation is based on the observation that $\mathcal{J}(r_{ab})$ defined in Eq. (97) selects from Eqs. (S1)–(S124) in the Supplemental Material [7] only terms proportional to $\hat{S}^z_a\hat{S}^z_b$. These terms we marked by ✠ symbols. There are 12 such terms, and the trace in Eq. (92) includes all of them.

Let $\hat{\boldsymbol{G}}^{+S^z_aS^z_b}$ be the sum of terms proportional to $\hat{S}^z_a\hat{S}^z_b$ and $\Omega^{S^z_aS^z_b}$ be the part of the grand canonical potential including $\hat{\boldsymbol{G}}^{+S^z_aS^z_b}$. Then, we have from Eqs. (95) and (96)

$$\Omega^{S^z_aS^z_b} = \frac{1}{\pi}\int_0^\infty dE \int_{-\infty}^{E} dE'\left[\mathrm{Im}\int \mathrm{Tr}\{\hat{\boldsymbol{G}}^{+S^z_aS^z_b}\}d^3\boldsymbol{r}\right]. \tag{99}$$

Calculating the sum of 12 components of $\hat{\boldsymbol{G}}^{+S^z_aS^z_b}$, and taking the explicit form of elements $\hat{q}^{1\alpha}$ and $\hat{q}^{2\alpha}$ matrices, with $\alpha = A, B, C, D$ [see Eqs. (S153)–(S192) in the Supplemental Material [7]], one obtains after some algebra

$$\Omega^{S^z_aS^z_b} = \Omega^{ab} + \Omega^{01} + \Omega^{02}. \tag{100}$$

By Ω^{ab} we denote the part of $\Omega^{S^z_aS^z_b}$ depending on the interspin distance r_{ab}, and by $\Omega^{01} + \Omega^{02}$ we denote the part of $\Omega^{S^z_aS^z_b}$ which does not depend on r_{ab}. The indices 1 and 2 in $\Omega^{01} + \Omega^{02}$ indicate powers of the coupling constant J entering into these expressions. Then, there is

$$\Omega^{ab} = \frac{J^2}{\pi}\hat{S}^z_a\hat{S}^z_b\,\mathrm{Im}\int_0^{E_F}\left[\int_{-\infty}^{E} g_{ab}h_{ab}\,\omega_{ab}dE'\right]dE, \tag{101}$$

where g_{ab} is the one-electron GF at points $\boldsymbol{r}_a$ and $\boldsymbol{r}_b$ [see Eq. (9)], and h_{ab} is defined in Eq. (93),

$$\omega_{ab} = \frac{16(2p_1^2 - 4p_1 - p_2 + 4)}{[8p_1(3p_2 - 4) - 9p_2^2 + 8(p_2 - 2)](4p_1 - p_2 - 4)}, \tag{102}$$

and p_1, p_2 are given in Eqs. (38) and (39). Similarly,

$$\Omega^{01} = \frac{J}{\pi}\hat{S}^z_a\hat{S}^z_b\,\mathrm{Im}\int_0^{E_F}\left[\int_{-\infty}^{E} h_0\,\omega_{01}dE'\right]dE, \tag{103}$$

$$\Omega^{02} = \frac{J^2}{\pi}\hat{S}^z_a\hat{S}^z_b\,\mathrm{Im}\int_0^{E_F}\left[\int_{-\infty}^{E} g_0h_0\,\omega_{02}dE'\right]dE, \tag{104}$$

in which

$$\omega_{01} = \frac{32[p_1(p_2 + 4) - 4p_2]}{[8p_1(3p_2 - 4) - 9p_2^2 + 8(p_2 - 2)](4p_1 - p_2 - 4)}, \tag{105}$$

$$\omega_{02} = \frac{-16(2p_1^2 - 4p_1 - p_2 + 4)}{[8p_1(3p_2 - 4) - 9p_2^2 + 8(p_2 - 2)](4p_1 - p_2 - 4)}, \tag{106}$$

and h_0 is given in Eq. (94).

First, we analyze Ω^{ab} term that gives the main contribution to the range function $\mathcal{J}(r_{ab})$. For small J, we may expand ω_{ab} in Taylor series. Assuming $p_2 = J^2p_2^{ab}$ [see Eq. (39)], one obtains

$$\begin{aligned}\omega_{ab} \simeq {} & 1 - Jg_0 + \frac{9}{8}J^2g_0^2 - \frac{17}{16}J^3g_0^3 \\ & + \frac{1}{32}J^4\left[35g_0^4 - 11g_0^2p_2^{ab} - 14\left(p_2^{ab}\right)^2\right]\dots.\end{aligned} \tag{107}$$

One observes the following from Eqs. (101)–(107): (i) By taking $\omega_{ab} = 1$ in Eq. (101) one obtains the range function of the RKKY interaction (see Appendix B). (ii) For arbitrary

ω_{ab}, as given in Eq. (102), the double integral in Eq. (101) may not be calculated analytically, so calculations are performed numerically (see Sec. X). (iii) Since g_0 does not depend on the distance r_{ab} between localized spins, the second, third, and fourth terms in Eq. (107) do not alter the spatial oscillations of Ω^{ab}, they only affect its amplitude. (iv) For small J the difference between the exact and RKKY range functions is on the order of $\pm 2p_1 = \pm J g_0$, and usually it is on the order of a few percent. (v) The first modification of spatial dependence of ω_{ab} appears in the fourth order of J. This term includes p_2^{ab} which depends on r_{ab} [see Eq. (39)]. (vi) Since $p_1 \propto J$ and $p_2 \propto J^2$, for $J \to \infty$ there is $\omega_{ab} \propto J^{-4}$ and $\Omega^{ab} \propto J^{-2}$, which vanishes for large $|J|$. The last result is counterintuitive since for large values of $|J|$ one expects no difference of $\Omega^{S_a^z S_b^z}$ in Eq. (100) for configurations having parallel and antiparallel localized spins. This issue can be clarified within our formalism (see Sec. VIII and Appendix C).

Analyzing Eqs. (103) and (104) we consider first the case of small J and expand ω_{01} and ω_{02} in Eqs. (105) and (106) in power series of J. One has

$$\omega_{01} \simeq J g_0 - J^2(g_0^2 + 4c_2)/2 + \cdots , \tag{108}$$

$$J g_0 \omega_{02} \simeq -J g_0 + J^2 g_0^2 + \cdots , \tag{109}$$

i.e., the terms linear in J cancel out and one has

$$\Omega^{01} + \Omega^{02} \simeq -\frac{2J^3}{\pi} \hat{S}_a^z \hat{S}_b^z \, \mathrm{Im} \int_0^{E_F} dE \int_{-\infty}^{E} h_0(c_2 + \cdots) dE'. \tag{110}$$

We conclude the following: (i) The terms $\Omega^{01} + \Omega^{02}$ are of the third order in the coupling constant J, while the Ω_{ab} term is of the second order in J. (ii) Contrary to Ω_{ab}, the terms $\Omega^{01} + \Omega^{02}$ include the product $g_0 h_0$ which does not depend on r_{ab}, and for this reason these terms weakly depend on the distance between spins. (iii) For large $|J|$ the sum $\Omega^{01} + \Omega^{02}$ vanishes as J^{-2}, similarly to Ω_{ab}. (iv) Physically, $\Omega^{01} + \Omega^{02}$ are generalization of the onsite energies appearing in the second order of perturbation expansion. Numerical calculations for 3D range function show that, for reasonable r_{ab}, the contribution of $\Omega^{01} + \Omega^{02}$ to the range function is a few orders of magnitude smaller than that of Ω^{ab} term. Therefore, the impact of $\Omega^{01} + \Omega^{02}$ terms on the range function may be neglected.

VIII. APPROXIMATE FORM OF Ω^{ab} IN 3D

Now we consider a simplified version of Eq. (102) in which we assume that the one-electron GF vanishes sufficiently fast with r_{ab}. This approximation works correctly for electrons in parabolic energy bands in 3D and 2D (see Sec. IX). Let

$$p_2 = \frac{J^2}{4}\left(g_0^2 - g_{ab} g_{ba}\right) \simeq \frac{J^2 g_0^2}{4} = p_1^2, \tag{111}$$

where $p_1 = J g_0/2$ [see Eq. (38)]. Then, from Eqs. (101), (102), and (111) one obtains

$$\Omega^{ab} \simeq \frac{16 J^2}{9\pi} \hat{S}_a^z \hat{S}_b^z \, \mathrm{Im} \int_0^{E_F} dE \int_{-\infty}^{E} \frac{g_{ab} h_{ab} \, dE'}{(p_1 - 2)^2 (p_1 + 2/3)^2} \tag{112}$$

and

$$\Omega^{01} + \Omega^{02} \simeq 0. \tag{113}$$

Equations (112) and (113) give a simple but complete description of the spin-dependent part of the thermodynamical potential and the range function $\mathcal{J}(r_{ab})$ in the whole range of model parameters. First, taking $p_1 \simeq 0$ one obtains

$$\Omega^{ab} \simeq \frac{J^2}{\pi} \hat{S}_a^z \hat{S}_b^z \, \mathrm{Im} \int_0^{E_F} dE \int_{-\infty}^{E} g_{ab} h_{ab} \, dE, \tag{114}$$

i.e., the thermodynamical potential and the range function for the RKKY interaction (see Appendix B). Next, for $0 \leqslant E \leqslant E_F$ the quantity g_0 entering p_1 is a nonoscillating slowly varying function of energy. Thus, for $p_1 \ll 2$ and $-p_1 \ll 2/3$ the denominators in Eq. (112) are also slowly varying functions of energy. These terms modify the amplitude of the range function but not its oscillations. For large $|p_1|$ and $|J|$ the denominators in Eq. (112) diminish the amplitude of range function and introduce an additional phase shift to the oscillations. For very large $|J|$ the range function vanishes as $|J|^{-2}$, as found previously. Finally, in the simplified model the one-site interactions do not give any contribution to the range function in full analogy to the RKKY case.

The quantity g_0 is a complex number: $g_0 = g_0^R + i g_0^I$. Usually, the real part of g_0 slowly varies with E, while g_0^I is proportional to the density of states of the system. For two values of J and appropriate energies there is $J g_0^R/2 \simeq 2$ or $J g_0^R/2 \simeq -2/3$, and the real part of $(p_1 - 2)$ or $(p_1 + 2/3)$ vanishes. Then, one of the denominators in Eq. (112) becomes large, especially for low energies. In this case, one may expect a significant enhancement of Ω^{ab} and consequently the range function $\mathcal{J}(r_{ab})$. This effect is quite general, but its magnitude depends on one-electron GF in the considered system.

The singular points of the integrand in Eq. (112) appear for $p_1 = 2$ or $-\frac{2}{3}$ and the vanishing imaginary part of g_0. In 3D this occurs for energies $E \leqslant 0$ since the density of states vanishes at or below the edge of the conduction band. For a specific combination of parameters, one may expect the presence of localized states with discrete energies. This issue is discussed in Sec. IX. Note that for the general case of Eq. (101) the singularities appear not exactly at $p_1 = 2$ or $-\frac{2}{3}$, but in the vicinity of these points because of the more complicated form of p_2 [see Eq. (39)].

The above considerations suggest the existence of three different regimes of parameters in the considered model. For small coupling constants J the exact range function resembles the RKKY one, with slightly altered amplitude but unchanged oscillation period. For parameters meeting the conditions $p_1 \simeq 2$ or $p_1 \simeq -\frac{2}{3}$ the thermodynamical potential Ω^{ab} and the range function $\mathcal{J}(r_{ab})$ are qualitatively different from the RKKY case and discrete energy states appear. The third regime occurs for large values of $|J|$ or $|g_0|$. In this case, the thermodynamic potential Ω^{ab} and the range functions resemble RKKY ones, but with additional phase shift in oscillations and much lower amplitude vanish with increasing $|J|$ or $|g_0|$. Numerical results in Sec. X confirm the above predictions.

Origin of model peculiarities

The approximations in Eqs. (111) and (112) allow us to understand three peculiar features of the exact GF, namely, (i) the asymmetry between positive (antiferromagnetic) and negative (ferromagnetic) signs of the coupling constant J, (ii) existence of two singularities for $Jg_0/2 \in \{2, -\frac{2}{3}\}$, and (iii) disappearance of the range function for large $|J|$ values. Below, we present the main steps in rederivation of the density of states entering the integrand of Eq. (112) in the approximate model and explain the mathematical and physical origins of the peculiarities.

Consistently with the approximation given in Eq. (111) we neglect in Eqs. (30) and (31) terms including products of $g_{ab}g_{ba}$. Then, from Eqs. (30) and (31) one obtains

$$\hat{\boldsymbol{Q}}_1 \simeq (\hat{I} - g_0\hat{\boldsymbol{Z}}_a)^{-1}(\hat{I} - g_0\hat{\boldsymbol{Z}}_b)^{-1} \equiv \hat{\boldsymbol{K}}_a\hat{\boldsymbol{K}}_b, \tag{115}$$

$$\hat{\boldsymbol{Q}}_2 \simeq (\hat{I} - g_0\hat{\boldsymbol{Z}}_b)^{-1}(\hat{I} - g_0\hat{\boldsymbol{Z}}_a)^{-1} \equiv \hat{\boldsymbol{K}}_b\hat{\boldsymbol{K}}_a. \tag{116}$$

In Eqs. (115) and (116) the quantities $\hat{\boldsymbol{K}}_a, \hat{\boldsymbol{K}}_b$ are 2×2 matrices, whose elements are combinations of $\hat{S}_a$ and $\hat{S}_b$ spin components (see below). For finite and nonzero g_0 there is

$$(\hat{I} - g_0\hat{\boldsymbol{Z}}_c)^{-1}\hat{\boldsymbol{Z}}_c = \frac{1}{g_0}(\hat{\boldsymbol{K}}_c - \hat{I}), \tag{117}$$

where $c = a, b$. Note that $(\hat{I} - g_0\hat{\boldsymbol{Z}}_c)$ commutes with $\hat{\boldsymbol{Z}}_c$. From Eq. (29) one has

$$\begin{aligned}\hat{\boldsymbol{G}}_{12} \simeq{}& g_{12}\hat{I} + \frac{g_{1a}}{g_0}(\hat{\boldsymbol{K}}_a - \hat{I})g_{a2} + \frac{g_{1b}}{g_0}[\hat{\boldsymbol{K}}_b - \hat{I}]g_{b2}\\ &+ \frac{g_{1a}}{g_0^2}[g_{ab}(\hat{\boldsymbol{K}}_a - \hat{I})(\hat{\boldsymbol{K}}_b - \hat{I})]g_{b2}\\ &+ \frac{g_{1b}}{g_0^2}[g_{ba}(\hat{\boldsymbol{K}}_b - \hat{I})(\hat{\boldsymbol{K}}_a - \hat{I})]g_{a2}.\end{aligned} \tag{118}$$

The first observation from Eqs. (115), (116), and (118) is that, for large $|J|$, the operators $\hat{\boldsymbol{K}}_a, \hat{\boldsymbol{K}}_b$ tend to zero and in this limit $\hat{\boldsymbol{G}}_{12}$ in Eq. (118) does not depend on $\hat{S}_a$ and $\hat{S}_b$. In consequence, the thermodynamic potential does not depend on spin configuration, so that the range function $\mathcal{J}(r_{ab})$ in Eq. (97) vanishes. The derivation of this result for the general case is shown in Appendix C.

The next conclusion from Eq. (118) is that, in the approximate model, the one-site parts of the exact GF, given by the two last terms of first line in Eq. (118), do not depend on the interspin distance r_{ab}. This observation suggests that also in the general model discussed in the previous sections, these terms are negligible.

The density of states is proportional to the trace of $\hat{\boldsymbol{G}}_{12}$. Let

$$\hat{\boldsymbol{K}}_c = \begin{pmatrix}\hat{k}^{cA} & \hat{k}^{cB}\\ \hat{k}^{cC} & \hat{k}^{cD}\end{pmatrix}, \tag{119}$$

with $c = a, b$. Using the notation from Sec. VI find $\mathrm{Tr}\{\hat{G}\} = \mathrm{Tr}\{\hat{G}_{ab}\} + \mathrm{Tr}\{\hat{G}_{ba}\}$, where

$$\begin{aligned}\mathrm{Tr}\{\hat{G}_{ab}\} ={}& \frac{g_{ab}h_{ab}}{g_0^2}(\hat{k}^{aA}\hat{k}^{bA} + \hat{k}^{aB}\hat{k}^{bC} + \hat{k}^{aC}\hat{k}^{bB} + \hat{k}^{aD}\hat{k}^{bD} - \hat{k}^{aA}\\ &- \hat{k}^{aD} - \hat{k}^{bA} - \hat{k}^{bD} + 2\hat{I}),\end{aligned} \tag{120}$$

$$\begin{aligned}\mathrm{Tr}\{\hat{G}_{ba}\} ={}& \frac{g_{ab}h_{ab}}{g_0^2}(\hat{k}^{bA}\hat{k}^{aA} + \hat{k}^{bB}\hat{k}^{aC} + \hat{k}^{bC}\hat{k}^{aB} + \hat{k}^{bD}\hat{k}^{aD} - \hat{k}^{bA}\\ &- \hat{k}^{bD} - \hat{k}^{aA} - \hat{k}^{aD} + 2\hat{I}).\end{aligned} \tag{121}$$

Equation (120) corresponds to the sum $(\hat{G}^{ab})_{11} + (\hat{G}^{ab})_{22}$ in Eqs. (50)–(65), while Eq. (121) corresponds to the sum $(\hat{G}^{ba})_{11} + (\hat{G}^{ba})_{22}$. The trace of GF obtained in Eqs. (120) and (121) is simpler than that in Eqs. (50)–(65). Using the Woodbury identities in Eq. (21) and definition of $\hat{\boldsymbol{K}}_c$ in Eqs. (115) and (116) one obtains

$$\hat{k}^{aA} = \left[(\hat{I} - p_1\hat{S}_a^z) - p_1^2\hat{S}_a^-\left(\hat{I} + p_1\hat{S}_a^z\right)^{-1}\hat{S}_a^+\right]^{-1}, \tag{122}$$

$$\hat{k}^{aD} = \left[\left(\hat{I} + p_1\hat{S}_a^z\right) - p_1^2\hat{S}_a^+\left(\hat{I} - p_1\hat{S}_a^z\right)^{-1}\hat{S}_a^-\right]^{-1}, \tag{123}$$

$$\hat{k}^{aB} = p_1\hat{k}^{aD}\hat{S}_a^-\left(\hat{I} + p_1\hat{S}_a^z\right)^{-1}, \tag{124}$$

$$\hat{k}^{aC} = p_1\hat{k}^{aA}\hat{S}_a^+\left(\hat{I} - p_1\hat{S}_a^z\right)^{-1}, \tag{125}$$

and similarly for $\hat{k}^{b\alpha}$ with $\alpha = A, B, C, D$. For the spins $\hat{S}_a, \hat{S}_b = \frac{1}{2}$ the operators $\hat{S}_a^\pm, \hat{S}_a^z, \hat{S}_b^\pm, \hat{S}_b^z$ are 4×4 matrices [see Eqs. (68) and (69)]. Then, the operators $\hat{k}^{a\alpha}$ and $\hat{k}^{b\alpha}$ are also 4×4 matrices that can be calculated from Eqs. (S204)–(S209) in the Supplemental Material [7].

Having calculated matrices $\hat{k}^{a\alpha}$ and $\hat{k}^{b\alpha}$ the trace in Eq. (120) in the Zeeman base (67) is

$$\mathrm{Tr}\{\hat{G}_{ab}\} = \frac{g_{ab}h_{ab}}{g_0^2}\begin{pmatrix}x_{11} & 0 & 0 & 0\\ 0 & x_{22} & x_{23} & 0\\ 0 & x_{32} & x_{33} & 0\\ 0 & 0 & 0 & x_{44}\end{pmatrix}, \tag{126}$$

and the x_{ij} are listed in Eqs. (S201)–(S203) in the Supplemental Material [7]. On the other hand, there is

$$\begin{aligned}\mathrm{Tr}\{\hat{G}_{ab}\} ={}& \frac{g_{ab}h_{ab}}{g_0^2}\big(c_1\hat{I} + c_2\hat{S}_a^z + c_3\hat{S}_b^z + c_4\hat{S}_a^z\hat{S}_b^z\\ &+ c_5\hat{S}_a^+\hat{S}_b^- + c_6\hat{S}_a^-\hat{S}_b^+\big),\end{aligned} \tag{127}$$

where c_i are coefficient to be determinate. The range function is defined as a coefficient c_4 in front of $\hat{S}_a^z\hat{S}_b^z$ [see Eq. (99)]. After some algebra we find $c_4 = x_{11} - x_{22} - x_{33} + x_{44}$, which gives

$$\mathrm{Tr}\left\{\hat{G}_{ab}^{\hat{S}_a^z\hat{S}_b^z}\right\} = \left(\frac{8J^2}{9\pi}\right)\frac{g_{ab}h_{ab}}{(p_1 - 2)^2(p_1 + 2/3)^2}. \tag{128}$$

Since $\mathrm{Tr}\{\hat{G}_{ba}^{\hat{S}_a^z\hat{S}_b^z}\} = \mathrm{Tr}\{\hat{G}_{ab}^{\hat{S}_a^z\hat{S}_b^z}\}$ one finally obtains $\mathrm{Tr}\{\hat{G}^{\hat{S}_a^z\hat{S}_b^z}\} = 2\,\mathrm{Tr}\{\hat{G}_{ab}^{\hat{S}_a^z\hat{S}_b^z}\}$, i.e., the integrand in Eq. (112). On expanding it around $p_1 = 0$ we find

$$\mathrm{Tr}\{\hat{G}^{\hat{S}_a^z\hat{S}_b^z}\} \simeq \frac{g_{ab}h_{ab}}{\pi}(1 - Jg_0 + \cdots), \tag{129}$$

i.e., the same expansion as in Eq. (107). This confirms the accuracy of the simplified form of thermodynamical potential in Eq. (112).

In the Zeeman basis (67) the matrix corresponding to $\hat{k}^{aA}$ operator in Eq. (122) is diagonal

$$\hat{k}^{aA} = \mathrm{diag}(k_2,\ k_2,\ k_2 + k_{-2/3},\ k_2 + k_{-2/3}), \tag{130}$$

with $k_2 = 1/(2-p_1)$ and $k_{-2/3} = 1/(3p_1+2)$. The matrix in Eq. (130) and the remaining matrices $\hat{k}^{a\alpha}$ and $\hat{k}^{b\alpha}$ have singularities for $p_1 \in \{2, -\frac{2}{3}\}$, i.e., for the same p_1 values as the singularities of the thermodynamical potential in Eq. (112). Thus, singularities of the exact GF appear when the operators $(\hat{I} - g_0\hat{\mathbf{Z}}_a)$ or $(\hat{I} - g_0\hat{\mathbf{Z}}_b)$ may not be inverted. For $\hat{S}_a, \hat{S}_b = \frac{1}{2}$ this occurs for two p_1 values: $p_1 = 2$ or $-\frac{2}{3}$. Since $p_1 = Jg_0/2$, the nonreversibility of $(\hat{I} - g_0\hat{\mathbf{Z}}_a)$ and $(\hat{I} - g_0\hat{\mathbf{Z}}_b)$ operators breaks the symmetry between positive (antiferromagnetic) and negative (ferromagnetic) values of J. This effect does not exist for the GF of the RKKY range function since the latter depends on J^2 and it is symmetric respect to positive or negative J values.

IX. ONE-ELECTRON GREEN'S FUNCTION

The results for GF in Eqs. (49)–(65) and (S1)–(S124) in the Supplemental Material [7] are valid for one-electron GF having arbitrary energy band dispersion but a finite value of g_0 [see Eq. (10)]. We consider electrons in the effective mass approximation in a parabolic energy band. The use of such GF allows us to compare the range function obtained from the exact GF with that obtained in the RKKY model.

A. Parabolic energy bands

Taking the Bloch states $|\boldsymbol{k}\rangle$ in the form of plane waves the one-electron GF in the effective mass approximation is

$$g_{ab} = \langle \boldsymbol{r}_a|\hat{g}|\boldsymbol{r}_b\rangle = \frac{1}{(2\pi)^D}\int \frac{e^{i\boldsymbol{k}(\boldsymbol{r}_a-\boldsymbol{r}_b)}}{E-\epsilon(k)}d^D\boldsymbol{k}, \tag{131}$$

$$\epsilon(k) = \frac{\hbar^2 k^2}{2m^*} \equiv \zeta k^2. \tag{132}$$

Here, D is the system's dimensionality, m^* is the electron effective mass, and $\zeta = \hbar^2/(2m^*)$. For $T = 0$ the energy E is a real number with a small imaginary part.

For 3D systems one has [18]

$$g^{\pm}_{ab} = -\frac{e^{ik_0 r_{ab}}}{4\pi r_{ab}\zeta}, \tag{133}$$

where $k_0 = \sqrt{|E|/\zeta} > 0$, $\mathrm{Re}(E) > 0$, $r_{ab} = |\boldsymbol{r}_a - \boldsymbol{r}_b|$, and $\pm$ signs correspond to the retarded and advanced Green's function, respectively. From Eqs. (93) and (94) one obtains

$$h^{+}_{ab} = \frac{ie^{ik_0 r_{ab}}}{8\pi k_0}, \tag{134}$$

$$h^{+}_{0} = \frac{i}{8\pi k_0}. \tag{135}$$

For 2D systems [18]

$$g^{\pm}_{ab} = -\frac{i}{4\pi\zeta}H_0(\pm k_0 r_{ab}), \tag{136}$$

where $H_0(x)$ is the zeroth-order Hankel function of the first kind. For the 1D systems [18]

$$g^{\pm}_{ab} = \mp\frac{i}{2k_0\zeta}e^{\pm ik_0 x_{ab}}. \tag{137}$$

As seen from Eqs. (133)–(137), the one-electron GF at the origin $g_0 = g_{11} = g_{22}$ diverges in $D = 3$ and $D = 2$. In 1D there is

$$g^{\pm}_{0} = \mp\frac{i}{2k_0\zeta}, \tag{138}$$

which is finite for $k_0 \neq 0$. These results conclude the issue of convergence of the perturbation series in the RKKY problem. As follows from the above consideration, the latter stated in its basic form leads to divergent perturbation series for 3D and 2D systems.

B. Cutoff energy

There exist several effects in real materials which may eliminate divergence of g_0. Here we consider one of these effects, i.e., a nonparabolicity of the energy band for large wave vectors. As seen in Eq. (133), the singularity of one-electron GF at $r_{ab} = 0$ arises from the divergence in the integral in Eq. (131) for large k, while for real materials the parabolic band dispersion is justified only for small k. For k exceeding, roughly, half of the first Brillouin zone, the curvatures of energy bands change their signs and the parabolic model fails.

To overcome the problem of divergence of g_0 for large k values, we follow the method described in Refs. [11–13]. For $\boldsymbol{r}_{ab} \neq 0$ we use the one-electron GF given in Eq. (131), while for $\boldsymbol{r}_{ab} = 0$ we take the GF in the energy representation

$$\begin{aligned} g^{+}_{0} &= \int_0^\infty \frac{n(E')}{E-E'+i\eta}dE' \\ &= \int_0^\infty \mathcal{P}\frac{n(E')}{E-E'}dE' - i\pi\int_0^\infty n(E')\delta(E-E')dE', \end{aligned} \tag{139}$$

where $n(E) \propto \sqrt{E}\,\Theta(E)$ is the density of states in 3D, $\Theta(E)$ is the step function, and $\mathcal{P}$ is the principal value of the integral. For large energies the real part of g^+_0 in Eq. (139) diverges. To remove this divergence, we introduce a cutoff energy $E_m \gg E_F$ that ensures convergence of the integrals in Eq. (139). We treat E_m as a model parameter. A similar approach of dealing with divergence of the one-electron GF was proposed in Ref. [19]. The density of states is then

$$n(E) = \frac{1}{2\pi^2\zeta^{3/2}}\sqrt{E}\;\Theta(E)\Theta(E_m - E). \tag{140}$$

For $E \geqslant 0$,

$$\begin{aligned} g^{+}_{0} &= \frac{1}{2\pi^2\zeta^{3/2}}\left[-\sqrt{E}\,\ln\left(\frac{\sqrt{E_m}-\sqrt{E}}{\sqrt{E_m}+\sqrt{E}}\right) - 2\sqrt{E_m}\right] \\ &\quad - \frac{i}{2\pi\zeta^{3/2}}\sqrt{E}\,\Theta(E_m - E), \end{aligned} \tag{141}$$

while for $E < 0$ there is

$$g^{+}_{0} = \frac{1}{2\pi^2\zeta^{3/2}}\left[2\sqrt{|E|}\arctan\left(\sqrt{\frac{E_m}{|E|}}\right) - 2\sqrt{E_m}\right], \tag{142}$$

since $n(E)$ is zero for $E < 0$. For $E \ll E_m$ the real part of g^+_0 is

$$\mathrm{Re}(g^{+}_{0}) \simeq \frac{1}{2\pi^2\zeta^{3/2}}\left(-2\sqrt{E_m} + \frac{E}{2E_m}\right) \text{ for } E \geqslant 0, \tag{143}$$

$$\mathrm{Re}(g_0^+) \simeq \frac{1}{2\pi^2\zeta^{3/2}}\left(-2\sqrt{E_m} + \pi\sqrt{|E|} - \frac{|E|}{2E_m}\right) \text{ for } E < 0. \tag{144}$$

For $E > 0$ the quantity g_0^+ is complex while for $E \leqslant 0$ it is real. We choose E_m as the energy at $k_m = \pi/a$, where a is the lattice constant. For many lattices as, e.g., for the fcc lattice in the ΓX direction of $\boldsymbol{k}$, the value of k_m corresponds to half of the Brillouin zone. Then,

$$E_m = \frac{\hbar^2\pi^2}{2m^*a^2}. \tag{145}$$

In 2D systems the real part of g_0^+ diverges as $\ln(E_m)$ and the results depend only weakly on E_m.

For $E = 0$ it is possible to adjust J, m^*, and E_m in such a way that $Jg_0^+/2 \in \{2, -\frac{2}{3}\}$. In the vicinities of these two points, the integral in Eq. (112) has two singularities. Using Eq. (145) and $\zeta = \hbar^2/(2m^*)$ we find that the two singularities appear for $p_1 = p_1^s$, where

$$p_1^s = -\frac{1}{2}\frac{J\sqrt{E_m}}{\pi^2\zeta^{3/2}} = -\frac{Jm^*}{\pi\hbar^2 a} \in \{2, -2/3\}. \tag{146}$$

The singularity $p_1 = 2$ occurs for negative values of J, i.e., for ferromagnetic coupling between conduction electrons and atomic d states. The singularity $p_1 = -\frac{2}{3}$ occurs for positive values of J, i.e., for antiferromagnetic s-d coupling. The two values of p_1^s indicate borders between three regimes of the model parameters. Their positions depend on electron effective mass, elementary cell volume, lattice constant, and s-d coupling constant. The two latter parameters do not change significantly between various compounds, but the effective mass may vary more than two orders of the magnitude. For narrow-gap semiconductors such as InSb, the effective mass can be below $0.1m_e$, while for some materials, e.g., $\mathrm{Sr}_{1-x}\mathrm{La}_x\mathrm{TiO}_{3-y}$, it can exceed $10m_e$. In many compounds it possible to change m^* by changing electron concentration or by applying external pressure. This may give a practical way of modifying p_1^s in Eq. (146).

C. Discrete energy levels

Discrete energy levels of a system are obtained from poles of $\hat{\boldsymbol{G}}_{12}$ function [18]. For the exact GF given in Eqs. (S1)–(S124) in the Supplemental Material [7], the poles of GF are obtained from two alternative equations

$$4p_1 - p_2 - 4 = 0, \tag{147}$$

$$32p_1^2(3p_2 - 4) - 4p_1\big(15p_2^2 + 8p_2 - 16\big) + (p_2 + 4)\big(9p_2^2 - 8p_2 + 16\big) = 0. \tag{148}$$

These equations are difficult to analyze and they can be solved only numerically. However, in 3D and 2D systems we may approximate $p_2 \simeq p_1^2$ [see Eq. (111)], and obtain instead of Eqs. (147) and (148) the condition $(p_1 - 2)(p_1 + 2/3) = 0$, which gives

$$\frac{Jg_0^+}{2} = 2 \quad \text{or} \quad \frac{Jg_0^+}{2} = -\frac{2}{3}. \tag{149}$$

For $E > 0$ and $E < E_m$ the conditions in Eq. (149) can not be satisfied. However, for $E \leqslant 0$ (i.e., below the conduction band edge) the imaginary part of g_0^+ vanishes and conditions in Eq. (149) may be satisfied for some combination of parameters entering to the model. Since we are interested in low-energy states, we use the approximate form of g_0^+ in Eq. (144). From (149) we have

$$\frac{J}{4\pi^2\zeta^{3/2}}(-2\sqrt{E_m} + \pi\sqrt{|E|}) = A, \tag{150}$$

where $A \in \{2, -\frac{2}{3}\}$. It is convenient to introduce

$$J^{\{A\}} = -\frac{2\pi^2\zeta^{3/2}A}{\sqrt{E_m}} \tag{151}$$

and $\delta J = J - J^{\{A\}}$. Assuming $\delta J \ll J^{\{A\}}$ one obtains from Eq. (150)

$$\sqrt{|E|} = \frac{4\pi A\zeta^{3/2}(J^{\{A\}} - J)}{J^{\{A\}}J} \simeq -\frac{4\pi A\zeta^{3/2}(\delta J)}{(J^{\{A\}})^2}. \tag{152}$$

The left-hand side of Eq. (152) is non-negative, which gives $-A(\delta J) \geqslant 0$. For $A = 2$ one obtains $(\delta J) < 0$. Since the singularity $A = 2$ corresponds to $J < 0$ [see the discussion after Eq. (146)], the bound states exist for $J \leqslant J^{\{2\}}$. For $A = -\frac{2}{3}$ there is $(\delta J) > 0$, and the bound states exist for $J \geqslant J^{\{-2/3\}}$. In both cases, the energies of bound states appear for small values of δJ in the vicinities of points $p_1 \in \{2, -\frac{2}{3}\}$.

X. NUMERICAL RESULTS

Here, we compare the range function $\mathcal{J}(r_{ab})$ of the standard RKKY interaction with that obtained in Eq. (97) with use of the exact GF and Eqs. (99)–(106). We restrict the analysis to the 3D case. The definite and indefinite integrals in Eqs. (101)–(104) are calculated by the Simpson method. To avoid singularities arising from $E = 0$, it is convenient to change the variable of integration $E \to q^2$. The model considered in this work depends on five parameters: s-d coupling constant J, values of localized spins $\hat{S}_a$, $\hat{S}_b$, electron effective mass m^*, the Fermi energy $E_F = \hbar^2k_F^2/(2m^*)$, and the cutoff energy E_m. In the 3D case the Fermi wave vector is

$$k_F = (3\pi^2 n_e)^{1/3}. \tag{153}$$

In Table I we list parameters corresponding to $\mathrm{ZnMn}_x\mathrm{Se}_{1-x}$, but with $\hat{S}_a, \hat{S}_b = \frac{1}{2}$ instead of $\hat{S}_a, \hat{S}_b = \frac{5}{2}$ [21,22]. These parameters are used in calculations shown in Figs. 1 and 3 and in Table II.

In Fig. 1 we plot values of the range function $\mathcal{J}$ for nearest-neighbor (NN) cations versus the coupling energy $\alpha N_0 = -J/\Omega_0$, where Ω_0 is the elementary cell volume. Note the sign convention in Eq. (6). The remaining material parameters are taken from Table I. The range function $\mathcal{J}_{\mathrm{RK}} \propto (\alpha N_0)^2$ is also indicated. This figure illustrates three regimes of model parameters discussed qualitatively in Sec. VII. The two extremes of the range function are located in the vicinities of $\alpha N_0 = -15.28$ eV, which corresponds to $p_1^s = -\frac{2}{3}$ [see Eqs. (146) and (112)] and $\alpha N_0 = 45.83$ eV corresponding to $p_1^s = 2$. Both values of αN_0 are more than two orders of magnitude larger than the experimental s-d coupling constant in $\mathrm{Zn}_{1-x}\mathrm{Mn}_x\mathrm{Se}$ (see Table I).

TABLE I. Material parameters for $Zn_{1-x}Mn_xSe$ used in calculations [21,22]. Note the sign convention in Eq. (6) and $\hat{S}_a, \hat{S}_b = \frac{1}{2}$ instead of $\hat{S}_a, \hat{S}_b = \frac{5}{2}$.

Parameter	Symbol	Value	Unit
Localized spin value	$\hat{S}_a, \hat{S}_b$	1/2	NA
s-d coupling constant	J	−11.85	eV Å^3
Lattice constant	a	5.67	Å
Effective mass	m^*	0.13	m_0
Electron concentration	n_e	6.0×10^{19}	cm^{-3}
Cutoff energy	E_m	8.99	eV
Elementary cell volume	Ω_0	45.57	Å^3
s-d coupling energy	$\alpha N_0 = -J/\Omega_0$	0.26	eV
Fermi vector	k_F	0.12	Å^{-1}
Fermi energy	E_F	0.43	eV
Parameter p_1^s	p_1^s	1.13%	NA

In Table II we compare the range functions calculated for several interspin distances r_{ab} using the exact GF with that obtained within RKKY formalism [see Eq. (4)] for $Zn_{1-x}Mn_xSe$ taking parameters from Table I with two signs of αN_0. The parameters correspond to regime I of the model that is most common in nature. The distance $r_{ab} = 4.01$ Å is the nearest-neighbor distance of Mn cations in the lattice. In our example, $p_1^s \simeq 1.13\%$. As follows from Eqs. (101) and (107), for small p_1^s the difference between exact and RKKY range functions should be on the order of $|Jg_0| \simeq |2p_1| \simeq 2.3\%$. Numbers shown in Table II confirm this expectation. The exact and approximate functions oscillate with similar period π/k_F and similar amplitudes. This result explains the efficiency and accuracy of the RKKY range function since for interspin distances larger than $r \geqslant 4$ Å, both models predict the same ordering of localized spins.

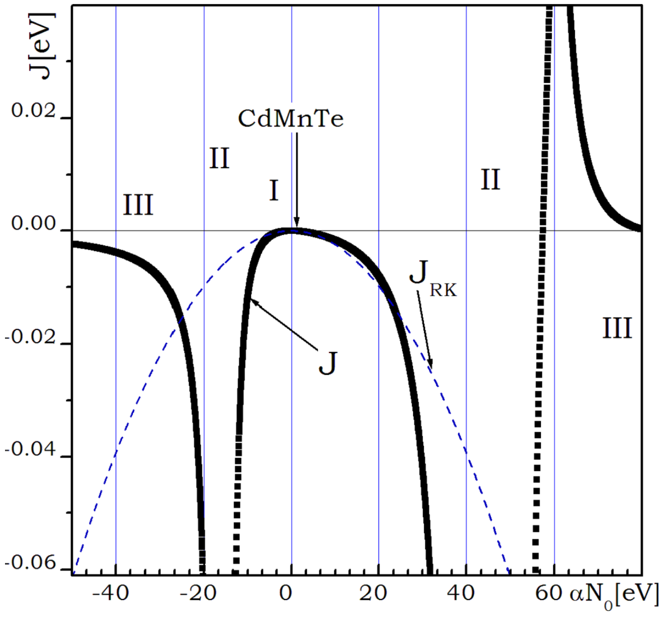

FIG. 1. Solid lines: amplitude of the range function $\mathcal{J}(r_{ab})$ calculated from Eqs. (97) and (99)–(106) versus αN_0 for NN cations distance $r_{ab} = 4.01$ Å. The remaining model parameters are listed in Table I. Three regimes of the model are marked. Dashed line: amplitude of the range function $\mathcal{J}_{RK}(r_{ab})$ from Eq. (4) versus αN_0 for $r_{ab} = 4.01$ Å.

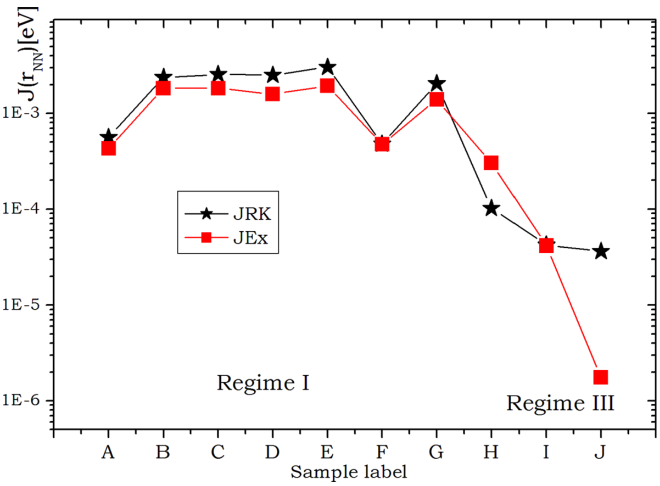

FIG. 2. Logarithms of $|\mathcal{J}_{RK}|$ given in Eq. (4) and exact range function $|\mathcal{J}|$ calculated using Eqs. (97) and (99)–(106) for nearest-neighbor magnetic impurities in $Sr_{1-x}La_xTiO_{3-\delta}$. Points are labeled according to Table III. The coupling constant between conduction and magnetic impurity electrons is ferromagnetic $J = -15.48$ eV Å^3. Results correspond to regimes I and III of model.

It follows from Eq. (146) that the regime III of the model occurs for large values of effective mass or large magnitude of the *s-d* coupling J. As an example of material in which the regime III may occur is thin film of $Sr_{1-x}La_xTiO_{3-\delta}$ doped with magnetic ions. This compound is one of perovskite-type transition-metal oxides in which the dispersion of electrons

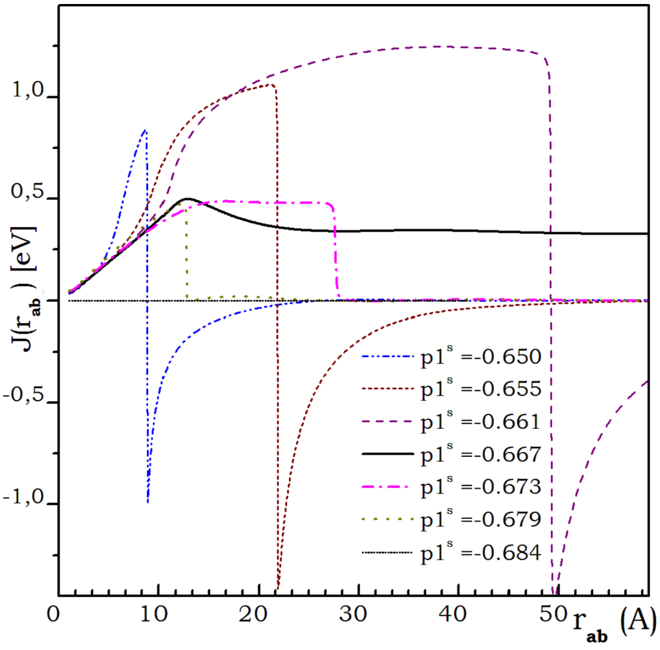

FIG. 3. Range function $\mathcal{J}(r_{ab})$ calculated exactly using Eqs. (97) and (99)–(106) in regime II of the model (see Fig. 1). Curves are labeled by values of p_1^s [see Eq. (146)]. The remaining parameters (except J and αN_0) are listed in Table I.

TABLE II. Values of RKKY range function $\mathcal{J}_{\rm RK}$ given in Eq. (4) and exact range function calculated using Eqs. (97) and (99)–(106) for $Zn_{1-x}Mn_xSe$ for several nearest-neighbor distances. Material parameters are given in Table I. Magnitudes of range functions are in μeV. The ± signs indicate positive (antiferromagnetic) or negative (ferromagnetic) sign of the *s*-*d* coupling constant J. In the last column: $\Delta^{\pm} = [\mathcal{J}^{\pm} - \mathcal{J}_{\rm RK}]/\mathcal{J}_{\rm RK}$ is the relative change of the exact range function. From Eq. (107) and Table I they should be $|\Delta^{\pm}| = 2|p_1| \simeq 2.3\%$.

r_{ab} (Å)	$\mathcal{J}(r_{ab})_{\rm RK}$	$\mathcal{J}(r_{ab})^-$	Δ^-
4.0	−2.599	−2.647	1.8%
5.7	−1.649	−1.681	1.9%
8.0	−0.960	−0.979	2.0%
11.3	−0.431	−0.439	1.9%
11.4	−0.420	−0.428	1.9%
r_{ab} (Å)	$\mathcal{J}(r_{ab})_{\rm RK}$	$\mathcal{J}(r_{ab})^+$	Δ^+
4.0	−2.599	−2.551	−1.8%
5.7	−1.649	−1.617	−2.0%
8.0	−0.960	−0.940	−2.0%
11.3	−0.431	−0.422	−2.1%
11.4	−0.420	−0.411	−2.1%

TABLE III. Values of RKKY range function $\mathcal{J}_{\rm RK}$ given in Eq. (4) and exact range function calculated using Eq. (97) and Eqs. (99)–(106) for nearest-neighbor magnetic impurities in $Sr_{1-x}La_xTiO_{3-\delta}$. The interspin distance is $r_{ab} = 3.905$ Å. Concentrations and effective masses are taken from Ref. [23], localized spins are $\hat{S}_a, \hat{S}_b = \frac{1}{2}$ and the coupling constant between conduction and magnetic impurity electrons is ferromagnetic $J = -15.48$ eV Å^3.

X	n_e (cm^{-3})	m^*/m_0	p_1^s	$\mathcal{J}_{\rm RK}$ (eV)	$\mathcal{J}$ (eV)
A	1.9×10^{20}	5.6	0.93	-5.60×10^{-4}	-4.29×10^{-4}
B	3.1×10^{21}	6.0	0.99	-2.39×10^{-3}	-1.84×10^{-3}
C	2.7×10^{21}	6.1	1.01	-2.56×10^{-3}	-1.84×10^{-3}
D	1.1×10^{21}	7.1	1.18	-2.52×10^{-3}	-1.59×10^{-3}
E	2.1×10^{21}	7.1	1.18	-3.05×10^{-3}	-1.95×10^{-3}
F	1.2×10^{20}	7.2	1.19	-4.40×10^{-4}	-4.74×10^{-4}
G	6.0×10^{20}	8.3	1.37	-2.05×10^{-3}	-1.40×10^{-3}
H	1.8×10^{19}	9.2	1.52	-1.02×10^{-4}	-3.02×10^{-4}
I	5.0×10^{18}	13.5	2.24	-4.23×10^{-5}	-4.18×10^{-5}
J	3.1×10^{18}	18.6	3.08	-3.66×10^{-5}	-1.76×10^{-6}

is parabolic with a large effective mass [24]. As shown in Ref. [23], by varying concentration of La atoms it is possible to change simultaneously the electron effective mass and carrier concentration. In our example it is assumed that a thin film of $Sr_{1-x}La_xTiO_{3-\delta}$ is doped with magnetic atoms having spin $\hat{S} = \frac{1}{2}$. We take the ferromagnetic coupling constant between conduction electrons and that of the magnetic impurity $J = -15.48$ eV Å^3. This corresponds to $\alpha N_0 = 0.26$ eV, i.e., to the experimental value for $Zn_{1-x}Mn_xSe$. Since the conduction band in $Sr_{1-x}La_xTiO_{3-\delta}$ is created mostly from the Ti $3d_{t2g}$ states, the parameter J may not be interpreted as the *s*-*d* coupling constant but as $3d$-f or $3d$-nd couplings. As follows from Refs. [25,26], for rare-earth atoms the exchange integrals are ferromagnetic with magnitudes of $J_{4f\text{-}5d} = -J/(2\Omega_0)$ [27] on the order of 180–140 meV depending on the number of electrons in the $4f$ shell, but other hybridization mechanisms lead to larger values of J.

In Table III and Fig. 2 we compare the exact and RKKY range functions for this films of $Sr_{1-x}La_xTiO_{3-\delta}$ doped with magnetic ions taking the effective mass and concentration from Ref. [23]. Parameter p_0^s is calculated from Eq. (146). Both range functions are calculated for $r_{ab} = a = 3.905$ Å, i.e., for the nearest-neighbor atoms. In this example the parameter p_1^s varies from 0.93 to 3.08, which corresponds to regimes I ($p_1^s < 2$) and III ($p_1^s > 2$) of the model (see Fig. 1). For p_1^s on the order of unity, the values of exact range function are a few times larger that those for the RKKY one. For larger p_1^s the exact range function is much smaller than the RKKY counterpart. For large p_1^s the ratio of exact range function to RKKY one is $(p_0^s)^{-4}$ [see Eq. (112)], and a similar ratio is obtained for $p_0^s = 3.08$. The results of Fig. 2 suggest a possible method to observe experimental deviation of the exact function $\mathcal{J}(r_{ab})$ from the RKKY one since by changing concentration of La atoms, both models predict significantly different values of coupling between neighboring magnetic impurities and, consequently, different Curie temperatures.

In Fig. 3 we plot the range function in the vicinity of $p_1^s = -\frac{2}{3}$, corresponding to $\alpha N_0 \simeq -15.28$ eV. In this regime the range function does not oscillate, and it has a very large amplitude. We present these results without detailed discussion because for parabolic energy bands the one-electron GF diverges at the origin and g_0 in Eq. (10) is infinite. The approximation of g_0 by a finite value gives reasonable results in two other regimes of parameters, but in the vicinities of singularities a more accurate one-electron GF is required.

Tables II and III and Figs. 2 and 3 provide three representative examples of the range function $\mathcal{J}(r_{ab})$ obtained from the exact GF. The behavior of $\mathcal{J}(r_{ab})$ confirms the qualitative description presented previously and, in particular, the predictions of the simplified model in Eq. (112).

XI. DISCUSSION

In the previous sections we described four main results for the exact GF of the system and the range function $\mathcal{J}(r_{ab})$. In Eqs. (49)–(65) the exact GF is expressed as a nonlinear combination of $\hat{S}_a, \hat{S}_b$ components and we provided a method of calculating the matrix elements of consecutive terms. These results are valid for arbitrary spin values but in practice such calculations can be done only numerically. For the spins $\hat{S}_a, \hat{S}_b = \frac{1}{2}$ we reexpressed the exact GF in terms of linear combinations of localized spins components [see Eqs. (S1)–(S124) in the Supplemental Material [7]] and calculated the exact range function [see Eqs. (97) and (99)–(106)]. The exact GF is obtained analytically, and the range function is found as integrals of analytical expressions [see Eqs. (101), (103), and (104)]. Both quantities depend on two dimensionless parameters p_1 and p_2 [see Eqs. (38) and (39)]. This form of GF and range function is still exact and suitable for numerical calculations, but it also does not explain the physical nature of the problem.

The third form of results is approximate and assumes that $p_2 \simeq p_1^2$ [see Eq. (111)]. This holds for one-electron GF vanishing sufficiently fast with the increasing distance $r_{ab} = |\boldsymbol{r}_a - \boldsymbol{r}_b|$. In practice, this is quite a good approximation in

3D systems and possibly in 2D systems. This approximation allows one to understand the three main physical features of the model: the existence of three regimes for small, large, and intermediate values of $|J|$, the asymmetry between ferromagnetic and antiferromagnetic values of s-d coupling constant, and possible existence of bound states corresponding to the poles of exact GF in the vicinities of points $p_1 \in \{2, -\frac{2}{3}\}$.

The fourth result is that the Born series is convergent if and only if the one-electron GF is finite at the origin. As a consequence, for the parabolic energy band dispersion in 3D and 2D systems, the Born series diverges, while in 1D it converges. Then, formally, the second-order GF in Eq. (1) and the range function in Eq. (4) are not sufficiently precise since one approximates the divergent series by a finite result. However, in real solids the parabolic energy approximation works roughly to half of the Brillouin zone and for larger wave vectors the band energies tend to a finite value. By taking a realistic band structure one introduces an energy cutoff related to a finite size of the Brillouin zone. Then, the one-electron GF at the origin is finite and the Born series converges. This reasoning restores the validity of RKKY results in Eq. (4) since after introducing the cutoff energy, one approximates the convergent Born series by its second-order term given in Eq. (1). Calculating the range function using GF approximated by this term one makes second approximation extending some energy integrals to the infinity, instead to the cutoff energy. Then, one finally obtains the analytical result for the range function in Eq. (4). We would like to mention that the s-d interaction is just the exchange part of the Coulomb interaction for which, as known, Born approximation gives correct experimental scattering amplitude even for parameters that violate formal convergence condition.

Since many issues related to the main results have been already discussed, here we only comment on the points related to other physical aspects of the considered problem. Calculations of the thermodynamic potential Ω in Eq. (95) and the range function in Eq. (97) can be also performed for finite temperatures. In this case, one should use the standard form of the Fermi-Dirac distribution function for finite T. Such calculations were reported in the literature for the RKKY case [28] and it turns out that at nonzero temperatures the oscillations have a similar period as for the $T = 0$ case, but the amplitude decreasing with temperature.

Calculating the one-electron GF in Eq. (131) with band energy in Eq. (132) one should take the velocity (or momentum) effective mass

$$\frac{1}{m^*} = \frac{1}{\hbar^2 k^2}\frac{d\epsilon(k)}{dk}. \tag{154}$$

This mass is well defined both for parabolic and nonparabolic energy bands. As discussed in Ref. [29], this effective mass can be obtained from cyclotron resonance experiments, dc transport phenomena, or free-carrier optics. In many systems there exists an anisotropy of the effective masses. In this case, one may not use an "average" or "density" effective mass, but one should calculate the one-electron GF in Eq. (133) taking into account this anisotropy.

In our approach we assumed that the potential of the crystal lattice does not mix electron states with different spins. Thus, in our considerations we neglect the spin-orbit interaction. This approximation is valid for electrons in conduction bands of metals or wide-gap semiconductors, but not for the holes, since usually the band structure of holes is strongly affected by the spin-orbit coupling. On the other hand, our model is valid for an arbitrary shape of electron bands. As an example, by taking the nonparabolic energy dispersion

$$\epsilon(\boldsymbol{k}) = \frac{\hbar^2 k^2}{2m^*}(1 \pm Ak^2), \tag{155}$$

where A is parameter of nonparabolicity, one obtains from Eqs. (10) and (131) a finite value of g_0. The same occurs for the tight-binding dispersion as, e.g.,

$$\epsilon(\boldsymbol{k}) = E_0 - t\,\cos(k_x a)\cos(k_y a)\cos(k_z a), \tag{156}$$

where E_0 and t are parameters of the tight-binding Hamiltonian. Then, the integration over $\boldsymbol{k}$ in Eq. (131) is restricted to the first Brillouin zone and one also obtains a finite value of g_0. The two above examples show that the existence of g_0 is a separate problem, independent of the derivation of the exact GF. In this work we considered parabolic energy bands because our intention was to compare the results obtained from the summation of the infinite series (exact GF) with results obtained for the lowest-order terms (RKKY model) in the parabolic approximation.

Our approach can be generalized to many energy bands and include the spin-orbit interaction. Assume for simplicity that one considers 2^j energy bands, where j is a positive integer. Then, in order to invert the operators $\hat{\boldsymbol{F}}_1$ and $\hat{\boldsymbol{F}}_2$ in Eqs. (30) and (31) one should apply the Woodbury identities $j + 1$ times [see Eqs. (21)–(23)]. In practice, it can be done only numerically. We expect that such a procedure gives similar results to those obtained in this paper.

The divergence of the perturbation series in 2D and 3D resembles difficulties arising for deltalike potentials for 2D and 3D systems. As discussed in [30], the presence of delta potential is inconsistent with the assumption that the electron wave function is finite at the origin. Such a problem does not exist in 1D or for systems with nonparabolic energy dispersion. Other peculiarities of singular potentials are discussed in Ref. [31].

Crucial assumption in our work is the zero-range potential in Eq. (6) since only for deltalike potentials the Dyson equation in Eq. (11) can be converted into algebraic equations. In practice, this potential is realized by two kinds of physical objects: atom nuclei or magnetic impurity atoms. The diameter of nucleus varies from 1.8 fm for hydrogen to about 11.7 fm for uranium. Both diameters are more than five orders of magnitude smaller than the lattice constant of metals, semiconductors, or heavy-fermion compounds. Therefore, the assumption of the zero-range potential is justified for all nuclear systems interacting with electrons in a crystal lattice [32]. The approximation of zero-range potential is less evident for magnetic moments occurring from the hybridization between d or f electrons of a magnetic impurity atom and band electrons [21]. The radius of an impurity atom is on the order of a half-lattice constant, which is typically around 3 Å. The period of oscillations of the range function is π/k_F, where $k_F \propto n_e^{1/3}$. The approximation of the s-d interaction by the δ-like potential is justified if $\pi/k_F \gg a/2$, which determines the maximum concentration of electrons in the sample.

The described model assumes presence of only two localized spins in the lattice. This assumption is valid for sufficiently diluted systems, as e.g. diluted magnetic or ferromagnetic semiconductors, in which one can disregard interactions between three or mores spins. But, there are systems like the Kondo lattice [33], in which all atoms (or cations) are coupled by the RKKY interaction, whose spatial decay is described by the standard formula for the RKKY range function. In these systems, the assumption of low-impurity concentration is not fulfilled both for the exact and the RKKY range functions. However, because of the fast decay of range functions with interspin distance, the presence of more distant magnetic atoms may be neglected. Nevertheless, some caution is needed when applying the results given in Figs. 2 and 3 to such systems.

An exponential decay of the RKKY interaction was proposed in literature to fit experimental values of the Curie temperature in some systems [34]. However, as explained in Ref. [35], the exponential decay of RKKY interaction results not from exponential form of the range function, but rather from averaging over random distribution of magnetic impurities in the lattice. The same arguments can be applied to the exact range function regimes I and III of the model because in these regimes the exact range function resembles the RKKY one.

In Ref. [36] we successfully removed the divergence of g_0 for the Friedel oscillations using the regularization procedure. This approach may not be applied in the present case because in the exact GF, there exist several divergent terms. In consequence, each term of GF should be regularized using different regulators, i.e., different values of J^{eff}. In this work we used a different approach and introduced only one effective parameter, namely, the cutoff energy E_m [see Eq. (131)]. Therefore, all terms of the exact GF are calculated using the same approximation.

The exact GF calculated in this work relates to the problem of two magnetic impurities interacting via *s-d* interaction. However, this is not a problem of two-impurity Anderson Hamiltonian. The reason is that the RKKY interaction, obtained in the second order of perturbation in terms of *s-d* coupling constant, differs from the interaction obtained in the fourth order of the V_{sd} hybridization parameter of the Anderson models since the latter includes some extra terms that are not present in RKKY [37]. The same terms are omitted in the calculation of the exact GF.

The results given in Eqs. (49)–(65) and (S1)–(S124) in the Supplemental Material [7], are valid for any system dimension D. The case of $D = 3$ was analyzed in previous sections, so here we briefly discuss the exact range function in one and two dimensions. In 2D systems the exact range function oscillates with the period $T = \pi/k_F$ and for large r_{ab} it vanishes as $1/r_{ab}^2$. We expect the existence of similar three regimes for small, intermediate, and large *s-d* coupling, analogous to those shown in Fig. 1. For parabolic energy bands in 2D the real part of g_0 diverges as $\ln(E)$ and in order to eliminate this divergence one also should add the cutoff energy E_m [see Eq. (141)]. But, because of the logarithmic divergence of $\text{Re}(g_0)$ in 2D, the quantity g_0 is less is sensitive to the cutoff energy than its counterpart in 3D. Finally, for large r_{ab} in 2D the one-electron GF in Eq. (136) decays as $1/r_{ab}^{0.5}$ and the approximate form of thermodynamical potential Ω_{ab} in Eq. (112) is less justified than in 3D.

In one dimension, the exact GF and the exact range function differ significantly from those in 3D and 2D. First, in 1D the quantity g_0 in Eq. (138) for a parabolic energy band is finite and imaginary. Next, the one-electron GF diverges for $E = 0$, and this singularity gives a nonzero contribution to the range function $\mathcal{J}(r_{ab})$ [38–40]. Because of the presence of the singularity, one may not decide about the existence of localized states. Finally, in 1D the one-electron GF in Eq. (137) oscillates in space with a constant amplitude, so the contributions of ω_{01} and ω_{02} terms in Eqs. (105) and (106) become comparable to that of ω_{ab}, while in 3D the contributions of ω_{01} and ω_{02} to the range function are negligible. However, it seems that there are no real 1D systems with electrons described by the effective mass approximation with spin-independent parabolic energy dispersion. For this reason we did not investigate the 1D case in more detail.

The method of calculating GF proposed in this work applies only to deltalike *s-d* interactions, and it can not be directly extended to models including exchange, correlations, screening, the presence of phonons, strain, etc. Nevertheless, it is possible to include these effects indirectly in a way similar to the RKKY interaction (see [4,10]). This method is based on the observation that the RKKY range function $\mathcal{J}_{\text{RK}}(r_{ab})$ is the Fourier transform of the susceptibility $\chi_0(\boldsymbol{q})$ of a free-electron gas

$$\mathcal{J}_{\text{RK}}(r_{ab}) = A_0 \sum_{\boldsymbol{q}} e^{i\boldsymbol{q}\boldsymbol{r}_{ab}} \chi_0(\boldsymbol{q}), \tag{157}$$

where A_0 is a constant. Then, one may replace in Eq. (157) the susceptibility $\chi_0(\boldsymbol{q})$ by the susceptibility $\chi(\boldsymbol{q})$ of electron gas calculated including many-body effects, nonlocal character of J, or screening. The same procedure can be applied to the exact range function $\mathcal{J}(r_{ab})$ in regimes I and III of the model since in these regimes the exact and the RKKY range functions differ by the scaling factor and the phase shift (see Table II and Fig. 2). In the regime II, the exact range function does not resemble the RKKY one (see Fig. 3), and there is no simple method of incorporating many-body effects to the range function.

In rare-earth materials the Coulomb exchange interaction between conduction electrons and $4f$-shell electrons is

$$\hat{V} = \sum_{\boldsymbol{k},\boldsymbol{k}'} -2J_{sf}(\boldsymbol{k},\boldsymbol{k}')(\acute{g}-1)\big(\hat{\boldsymbol{J}}_a + \hat{\boldsymbol{J}}_b\big)\hat{\boldsymbol{s}}, \tag{158}$$

where $\hat{\boldsymbol{J}}$ is the operator of the total angular momentum of $4f$ electrons and $\acute{g}$ is the Lande factor [41]. This approximation is valid if the wavelength of the conduction electron is large compared with the size of the $4f$ shell and if one neglects the dependence of the electron wave function on the direction in space. Our approach can be directly used to systems with the exchange potential given in Eq. (158) if the integral $J_{sf}(\boldsymbol{k},\boldsymbol{k}')$ may be approximated by the delta function. This could be valid for low electron concentrations resulting in large periods π/k_F of RKKY oscillations. When the exchange parameter $J(\boldsymbol{k},\boldsymbol{k}')$ can be approximated by $J_{sf}(\boldsymbol{q})$ with $\boldsymbol{q} = \boldsymbol{k} - \boldsymbol{k}'$, we may apply the spin susceptibility formalism from Eq. (157)

and make a substitution

$$\chi_0(\boldsymbol{q}) \to (\acute{g}-1)^2|J_{sf}(\boldsymbol{q})|^2\chi(\boldsymbol{q}). \tag{159}$$

This method may be used for $\mathcal{J}(r_{ab})$ in regimes I and III of parameters shown in Fig. 1.

In modern approaches, the RKKY range function are obtained with use of Lloyd's formula [42], which gives the difference between integrated densities of states $N(E)$ [see Eq. (96)] obtained from $\hat{g}(E)$ and $\hat{G}(E)$:

$$\Delta N(E) = -\frac{1}{\pi}\mathrm{Im}\mathrm{Tr}\ln(1-\hat{g}(E)\hat{V}_a-\hat{g}(E)\hat{V}_b), \tag{160}$$

where $\hat{V}_a, \hat{V}_b$ are given in Eq. (6) [43]. The identity (160) is exact for arbitrary $\hat{g}(E)$ and external potentials. The problem with Eq. (6) is how to evaluate the logarithm for operators $\hat{V}_a, \hat{V}_b$ having noncommuting components. In Eqs. (50)–(65) and (S1)–(S124) in the Supplemental Material [7] we calculated the exact GF of the system, and we may obtain $N(E)$ in Eq. (96) by taking the trace over the GF and performing the indefinite integration of $n(E)$ over the energy. Then, the results in Eq. (96) should be equal to the expression of the right-hand side of Eq. (160).

However, there are two differences between our approach and Lloyd's formula. First, the exact GF in Eqs. (50)–(65) and (S1)–(S124) in the Supplemental Material [7] is more general than the intergraded electron density in Eq. (160). For the calculation of thermodynamic properties of the system, which depend on electron densities $n(E)$ or $N(E)$, the Lloyd's formula may be more convenient than our approach. However, if one calculates quantities depending on the GF of the system, e.g., discrete energy states (as in Sec. IX) or the conductivity tensor, the knowledge of GF is necessary. Second, our approach is limited to deltalike potentials, while the Lloyd's formula is valid for arbitrary potentials and, within this formalism, one can include more physical effects (screening, phonons, etc.) than by our approach. However, Lloyd's approach requires calculation of the logarithm of noncommuting operators in Eq. (160) which in practice can be done only by the perturbation expansion.

The *s-d* coupling constant J in Eq. (6) is expressed in eV Å^D, where D is the system dimensionality. Experimentally, one measures the coupling constants J_{sd}, J_{sf}, J_{df}, etc., expressed in eV. They are related to J in Eq. (6): $J = -J_{sd}\Omega_0$, where Ω_0 is the elementary cell volume and the minus sign follows from sign convention in Eq. (6). In the theory of diluted magnetic semiconductors one uses notation $J_{sd} = \alpha N_0$ and $N_0 = 1/\Omega_0$ [21].

To observe experimentally a deviation of $\mathcal{J}(r_{ab})$ in Eqs. (100)–(106) from the RKKY range function in Eq. (4), one should meet the following conditions. First, both the *s-d* coupling J and the range function should be measured independently with sufficient accuracy. Second, the exchange, correlation, and screening terms in Eqs. (157), and (159) should be small. Finally, proper value of g_0 in the material should be known.

It seems difficult to observe the difference between two range functions in systems belonging to the regime I of parameters (see Table II) since in this case the difference between the exact and approximate range functions is on the order of $\pm 2p_1$, which is typically a few percent. In practice, such a small difference makes it impossible to distinguish experimentally between the two cases. A more promising way of experimental verification of the results given in Sec. X is the regime III in Fig. 2. In the latter, characterized by large *s-d* coupling $|J|$ or large effective mass [see Eq. (146)], there is significant difference between magnitudes of the exact and RKKY range functions. In consequence, by measuring independently the coupling constant J and the range function $\mathcal{J}(r_{ab})$, it should be possible to distinguish between the exact and approximate range functions even in the presence of additional terms in the generalized susceptibility of Eq. (159). Another promising way to confirm the results obtained in this work is to observe the bound states predicted in Sec. IX. Experimental difficulty in such measurements is the narrow range of parameters for which there should exist bound states.

XII. SUMMARY

The Green's function and the range function of two localized spins in electron gas is calculated exactly by summing the Born series using a generalization of the method of Slater-Koster and Ziman to noncommuting spin operators. Our calculations generalize the RKKY results that are obtained from the second-order terms of the Born series. We obtained four specific results. First, the exact GF is expressed as a nonlinear combination of localized spin components. This form of exact GF is valid for arbitrary spins. Second, for spins $\frac{1}{2}$ we reexpressed the exact GF as a linear combination of localized spin components. Third, an approximation is proposed for the exact GF that clearly explains the physical nature of the problem. Fourth, it is shown that the Born series converges if and only if the one-electron GF at the origin g_0 is finite. This occurs for electrons in parabolic energy bands in 1D but not in 2D or 3D. However, by introducing a proper cutoff energy in the calculation of one-electron GF, one obtains finite value of g_0 and the convergent Born series.

For spins $\hat{S}_a, \hat{S}_b = \frac{1}{2}$ there are three regimes of the model. For $|J| \ll |g_0|^{-1}$, the range function $\mathcal{J}_{3D}(r_{ab})$ resembles the RKKY one: it has the same period π/k_F, the same decay character, and a slightly different amplitude, usually differing by a few percent. This regime occurs most frequently in nature. For $|J|$ comparable to $|g_0|^{-1}$, the exact range function differs qualitatively from the RKKY one: it has a much larger amplitude, nonoscillatory character, and it decays more slowly with interspin distance. For $|J| \gg |g_0|^{-1}$ the exact range function oscillates with the same period and powerlike decay as the RKKY one, but it has much lower amplitude decreasing with growing $|J|$. In the limiting case $|J| \to \infty$, the range function vanishes.

For the electron energy $E = 0$ and $p_1 \simeq 2$ or $p_1 \simeq -\frac{2}{3}$ [see Eq. (112)], the range function and GF are singular, the poles of GF occur in the vicinities of the singularity points. The energies of bound states are calculated. In contrast to the standard RKKY approach, for the exact GF and the range function there is no symmetry between ferromagnetic and antiferromagnetic values of *s-d* coupling constant J. The asymmetry follows from the singularities of the operators $(\hat{I} - p_1\hat{\boldsymbol{Z}}_c)^{-1}$ for $p_1 \in \{2, -\frac{2}{3}\}$. We calculated the exact range function for one representative material using realistic model parameters. We also report results for the exact range function

$\mathcal{J}(r_{ab})$ in the wide range of values of s-d coupling constants J. We compared our results with other theoretical approaches existing in the literature. Promising ways to confirm experientially the results of this work are as follows: (i) independent measurement of the s-d coupling constant J and the range function $\mathcal{J}(r_{ab})$ in the regime $|J| \gg |g_0|^{-1}$ because there the amplitude of exact range function significantly differs from its RKKY counterpart; (ii) detection of bound states in the vicinities of points $p_1 \in \{2, -\frac{2}{3}\}$. We hope that the exact results reported in this paper will be useful in analyses of similar problems.

APPENDIX A: WOODBURY IDENTITIES

In this Appendix we prove the Woodbury identities used in Sec. II. They differ slightly from those given in Ref. [16]. First we prove Eq. (21), i.e., show that

$$\begin{bmatrix} \hat{\boldsymbol{\Delta}}_1^{-1} & -\hat{\boldsymbol{\Delta}}_1^{-1}\hat{\boldsymbol{B}}\hat{\boldsymbol{D}}^{-1} \\ -\hat{\boldsymbol{\Delta}}_2^{-1}\hat{\boldsymbol{C}}\hat{\boldsymbol{A}}^{-1} & \hat{\boldsymbol{\Delta}}_2^{-1} \end{bmatrix} \cdot \begin{bmatrix} \hat{\boldsymbol{A}} & \hat{\boldsymbol{B}} \\ \hat{\boldsymbol{C}} & \hat{\boldsymbol{D}} \end{bmatrix} = \begin{bmatrix} \hat{\mathbf{1}} & \hat{\mathbf{0}} \\ \hat{\mathbf{0}} & \hat{\mathbf{1}} \end{bmatrix}, \tag{A1}$$

with $\hat{\boldsymbol{\Delta}}_1$ and $\hat{\boldsymbol{\Delta}}_2$ defined in Eqs. (22) and (23), respectively. We have then

$$\hat{\boldsymbol{\Delta}}_1^{-1}\hat{\boldsymbol{A}} - \hat{\boldsymbol{\Delta}}_1^{-1}\hat{\boldsymbol{B}}\hat{\boldsymbol{D}}^{-1}\hat{\boldsymbol{C}} = \hat{\boldsymbol{\Delta}}_1^{-1}(\hat{\boldsymbol{A}} - \hat{\boldsymbol{B}}\hat{\boldsymbol{D}}^{-1}\hat{\boldsymbol{C}}) = \hat{\boldsymbol{\Delta}}_1^{-1}\hat{\boldsymbol{\Delta}}_1 = \hat{\mathbf{1}}. \tag{A2}$$

Similarly,

$$-\hat{\boldsymbol{\Delta}}_2^{-1}\hat{\boldsymbol{C}}\hat{\boldsymbol{A}}^{-1}\hat{\boldsymbol{B}} + \hat{\boldsymbol{\Delta}}_2^{-1}\hat{\boldsymbol{D}} = \hat{\boldsymbol{\Delta}}_2^{-1}(\hat{\boldsymbol{D}} - \hat{\boldsymbol{C}}\hat{\boldsymbol{A}}^{-1}\hat{\boldsymbol{B}}) = \hat{\boldsymbol{\Delta}}_2^{-1}\hat{\boldsymbol{\Delta}}_2 = \hat{\mathbf{1}}. \tag{A3}$$

Finally,

$$\hat{\boldsymbol{\Delta}}_1^{-1}\hat{\boldsymbol{B}} - \hat{\boldsymbol{\Delta}}_1^{-1}\hat{\boldsymbol{B}}\hat{\boldsymbol{D}}^{-1}\hat{\boldsymbol{D}} = \hat{\boldsymbol{\Delta}}_1^{-1}\hat{\boldsymbol{B}} - \hat{\boldsymbol{\Delta}}_1^{-1}\hat{\boldsymbol{B}} = \hat{\mathbf{0}}, \tag{A4}$$

$$-\hat{\boldsymbol{\Delta}}_2^{-1}\hat{\boldsymbol{C}}\hat{\boldsymbol{A}}^{-1}\hat{\boldsymbol{A}} + \hat{\boldsymbol{\Delta}}_2^{-1}\hat{\boldsymbol{C}} = -\hat{\boldsymbol{\Delta}}_2^{-1}\hat{\boldsymbol{C}} + \hat{\boldsymbol{\Delta}}_2^{-1}\hat{\boldsymbol{C}} = \hat{\mathbf{0}}. \tag{A5}$$

This proves Eq. (21). Now, we prove Eq. (26) for $[\hat{\boldsymbol{A}}, \hat{\boldsymbol{C}}] = 0$ and $[\hat{\boldsymbol{B}}, \hat{\boldsymbol{D}}] = 0$. There is

$$\begin{aligned} \hat{\boldsymbol{\Delta}}_1^{-1} &= (\hat{\boldsymbol{A}} - \hat{\boldsymbol{B}}\hat{\boldsymbol{D}}^{-1}\hat{\boldsymbol{C}})^{-1} = (\hat{\boldsymbol{D}}^{-1}\hat{\boldsymbol{D}}\hat{\boldsymbol{A}} - \hat{\boldsymbol{D}}^{-1}\hat{\boldsymbol{B}}\hat{\boldsymbol{C}})^{-1} \\ &= [\hat{\boldsymbol{D}}^{-1}(\hat{\boldsymbol{D}}\hat{\boldsymbol{A}} - \hat{\boldsymbol{B}}\hat{\boldsymbol{C}})]^{-1} = \hat{\boldsymbol{F}}_1^{-1}\hat{\boldsymbol{D}}, \end{aligned} \tag{A6}$$

$$\begin{aligned} \hat{\boldsymbol{\Delta}}_2^{-1} &= (\hat{\boldsymbol{D}} - \hat{\boldsymbol{C}}\hat{\boldsymbol{A}}^{-1}\hat{\boldsymbol{B}})^{-1} = (\hat{\boldsymbol{A}}^{-1}\hat{\boldsymbol{A}}\hat{\boldsymbol{D}} - \hat{\boldsymbol{A}}^{-1}\hat{\boldsymbol{C}}\hat{\boldsymbol{B}})^{-1} \\ &= [\hat{\boldsymbol{A}}^{-1}(\hat{\boldsymbol{A}}\hat{\boldsymbol{D}} - \hat{\boldsymbol{C}}\hat{\boldsymbol{B}})]^{-1} = \hat{\boldsymbol{F}}_2^{-1}\hat{\boldsymbol{A}}, \end{aligned} \tag{A7}$$

$$-\hat{\boldsymbol{\Delta}}_1^{-1}\hat{\boldsymbol{B}}\hat{\boldsymbol{D}}^{-1} = \hat{\boldsymbol{F}}_1^{-1}\hat{\boldsymbol{D}}\hat{\boldsymbol{B}}\hat{\boldsymbol{D}}^{-1} = \hat{\boldsymbol{F}}_1^{-1}\hat{\boldsymbol{B}}, \tag{A8}$$

$$-\hat{\boldsymbol{\Delta}}_2^{-1}\hat{\boldsymbol{C}}\hat{\boldsymbol{A}}^{-1} = \hat{\boldsymbol{F}}_2^{-1}\hat{\boldsymbol{A}}\hat{\boldsymbol{C}}\hat{\boldsymbol{A}}^{-1} = \hat{\boldsymbol{F}}_1^{-1}\hat{\boldsymbol{C}}. \tag{A9}$$

This completes the proof.

APPENDIX B: RKKY RANGE FUNCTION: $\omega_{ab} \simeq 1$

Here, we calculate the range function $\mathcal{J}_{\rm RK}(r_{ab})$ for the grand canonical potential Ω^{ab} in Eq. (101) in the limit $\omega_{ab} = 1$, i.e., by truncating the Born series to the terms of the second order in the s-d coupling constant J. We begin with Eq. (1), i.e., from the lowest-order terms of the Born series including both $\hat{V}_a$ and $\hat{V}_b$ potentials. Using the notation introduced in Sec. IV one obtains from Eq. (1)

$$\hat{\boldsymbol{G}}_{1,2}^{ab} \simeq g_{1a}\hat{\mathbf{Z}}_a g_{ab}\hat{\mathbf{Z}}_b g_{b2} + g_{1b}\hat{\mathbf{Z}}_b g_{ba}\hat{\mathbf{Z}}_a g_{a2}. \tag{B1}$$

Since $g_{ab} = g_{ba}$ one gets for the trace of $\hat{\boldsymbol{G}}_{1,2}^{ab}$

$$\begin{aligned} {\rm Tr}\{\hat{\boldsymbol{G}}_{1,2}^{ab}\} &= \left(\int d^3\boldsymbol{r}_1 g_{1a} g_{b1} g_{ab}\right){\rm Tr}\{\hat{\mathbf{Z}}_a\hat{\mathbf{Z}}_b + \hat{\mathbf{Z}}_b\hat{\mathbf{Z}}_b\} \\ &= J^2 g_{ab} h_{ab} \hat{\mathrm{S}}_a \hat{\mathrm{S}}_b. \end{aligned} \tag{B2}$$

Then, the $S_a^z S_b^z$ part of the thermodynamic potential is

$$\Omega^{ab} = \frac{J^2}{\pi}\hat{\mathrm{S}}_a^z\hat{\mathrm{S}}_b^z \int_0^{E_F}\left[\int g_{ab} h_{ab}\, dE'\right] dE, \tag{B3}$$

which is the limit given in Eq. (101) for $\omega_{ab} = 1$. Using the retarded one-electron GF

$$g_{ab}^{+} \equiv g_{ab} = -\frac{\exp(ir_{ab}\sqrt{E/\zeta})}{4\pi\zeta r_{ab}}, \tag{B4}$$

with $\zeta = \hbar^2/(2m^*)$, one obtains from Eq. (93)

$$h_{ab} = -\frac{dg_{ab}}{dE} = -\frac{\exp(ir_{ab}\sqrt{E/\zeta})}{8\pi\zeta^{3/2}\sqrt{E}}. \tag{B5}$$

The one-electron density of states $n(E)$ in Eq. (91) is then

$$n(E) = \frac{\cos(2r_{ab}\sqrt{E/\zeta})}{32\pi^3\zeta^{5/2}\sqrt{E}r_{ab}}. \tag{B6}$$

Calculating the double integral in Eq. (B3) with g_{ab}^{+} and h_{ab} given in Eqs. (B4) and (B5) and taking $k_F = \sqrt{E_F/\zeta}$ we find

$$\mathcal{J}_{\rm RK}(r_{ab}) = \frac{J^2}{64\pi^3 r_{ab}^4\zeta}[2r_{ab}k_F\cos(2k_F r_{ab}) - \sin(2k_F r_{ab})], \tag{B7}$$

which is the RKKY range function for electrons in a parabolic energy band in 3D.

APPENDIX C: GF AND RANGE FUNCTION FOR STRONG COUPLING

Consider the exact GF for large s-d coupling J. In this limit we approximate in Eqs. (30) and (31)

$$\hat{I} - g_0\hat{\mathbf{Z}}_c \simeq -g_0\hat{\mathbf{Z}}_c, \tag{C1}$$

where $c = a, b$. Then, we have

$$\hat{\boldsymbol{F}}_1 \simeq (g_0^2 - g_{ab}g_{ba})\hat{\mathbf{Z}}_b\hat{\mathbf{Z}}_a = z_{ab}\hat{\mathbf{Z}}_b\hat{\mathbf{Z}}_a, \tag{C2}$$

$$\hat{\boldsymbol{F}}_2 \simeq (g_0^2 - g_{ab}g_{ba})\hat{\mathbf{Z}}_a\hat{\mathbf{Z}}_b = z_{ab}\hat{\mathbf{Z}}_b\hat{\mathbf{Z}}_a, \tag{C3}$$

where $z_{ab} = g_0^2 - g_{ab}g_{ba}$ [see Eq. (39)]. In consequence, there is

$$\hat{\boldsymbol{Q}}_1 = \hat{\boldsymbol{F}}_1^{-1} \simeq \hat{\mathbf{Z}}_a^{-1}\hat{\mathbf{Z}}_b^{-1}/z_{ab}, \tag{C4}$$

$$\hat{\boldsymbol{Q}}_2 = \hat{\boldsymbol{F}}_2^{-1} \simeq \hat{\mathbf{Z}}_b^{-1}\hat{\mathbf{Z}}_a^{-1}/z_{ab}. \tag{C5}$$

From Eq. (29) one obtains

$$\begin{aligned} \hat{\boldsymbol{G}}_{12} \simeq{} & g_{12}\hat{I} + g_{1a}[\hat{\mathbf{Z}}_a\hat{\boldsymbol{Q}}_1(-g_0\hat{\mathbf{Z}}_b)]g_{a2} + g_{1a}[g_{ab}\hat{\mathbf{Z}}_a\hat{\boldsymbol{Q}}_1\hat{\mathbf{Z}}_b]g_{b2} \\ & + g_{1b}[g_{ba}\hat{\mathbf{Z}}_b\hat{\boldsymbol{Q}}_2\hat{\mathbf{Z}}_a]g_{a2} + g_{1b}[\hat{\mathbf{Z}}_b\hat{\boldsymbol{Q}}_2(-g_0\hat{\mathbf{Z}}_a)]g_{b2}. \end{aligned} \tag{C6}$$

Inserting the approximate forms of $\hat{\boldsymbol{Q}}_1$, $\hat{\boldsymbol{Q}}_2$ into Eq. (C6) one finally obtains

$$\hat{\boldsymbol{G}}_{12} \simeq g_{12}\hat{I} + \frac{1}{z_{ab}}(-g_0 g_{1a} g_{a2} + g_{ab} g_{1a} g_{b2} + g_{ba} g_{1b} g_{a2} - g_0 g_{1b} g_{b2}). \tag{C7}$$

As seen from Eq. (C7), for large J the GF does not depend on $\boldsymbol{S}_1$ and $\boldsymbol{S}_2$, and it has a universal character. Such behavior of GF for large perturbing potentials is known in the literature [36] and it appears even in simple models of one spinless impurity [see Eq. (5)].

The range function of the RKKY interaction is defined as a difference of the grand canonical potential for parallel and antiparallel spins [see Eq. (97)]. However, since the electron density $n_e \propto \mathrm{Im}\{\mathrm{Tr}(\hat{\boldsymbol{G}}_{12})\}$, as given in Eq. (C7), does not depend on $\boldsymbol{S}_1$ and $\boldsymbol{S}_2$, the grand canonical potential $\Omega_{\mu,\nu}$ in Eq. (98) also does not depend on spin configuration. The range function in Eq. (97) is a sum of two positive and two negative terms. For large $|J|$ all the four terms tend to a common value not depending on spin configurations. Thus, for large $|J|$ the range function $\mathcal{J}(r_{ab})$ vanishes, which explains the disappearance of the ω_{ab} term in Eq. (102) for large $|J|$.

---

[1] M. A. Ruderman and C. Kittel, Phys. Rev. **96**, 99 (1954).

[2] T. Kasuya, Prog. Theor. Phys. **16**, 45 (1956).

[3] K. Yosida, Phys. Rev. **106**, 893 (1957).

[4] A. J. Freeman, in *Magnetic Properties of Rare-Earth Metals*, edited by R. J. Elliott (Plenum, London, 1972), p. 245.

[5] C. Kittel, *Quantum Theory of Solids*, 2nd ed. (Wiley, New York, 1987).

[6] G. F. Koster and J. C. Slater, Phys. Rev. **96**, 1208 (1954).

[7] See Supplemental Material at http://link.aps.org/supplemental/10.1103/PhysRevB.101.205201 for formulas for the exact GF for $\hat{S}_a$, $\hat{S}_b = 1/2$ obtained from Eqs. (50)–(65)with use of a method described in Section VI. The terms proportional to products $\hat{S}^z_a\hat{S}^z_b$ are marked by ✠ symbol. We list elements of matrices corresponding to $\hat{f}^{1\alpha}$ and $\hat{f}^{2\alpha}$ operators ($\alpha = A, B, C, D$) defined in Eqs. (34)–(37), elements of matrices $\hat{q}^{1\alpha}$ and $\hat{q}^{2\alpha}$ defined in Eqs. (40)–(47), coefficients x_{ij} in Eq. (126) and elements of matrices $\hat{k}^{a\alpha}$, $\hat{k}^{b\alpha}$ in Eqs. (119) and (122)–(125).

[8] G. Vertogen and W. J. Gaspers, Phys. Rev. Lett. **16**, 904 (1966).

[9] S. P. Bowen, Phys. Rev. Lett. **20**, 726 (1968).

[10] C. Kittel, in *Solid State Physics*, edited by F. Seitz, D. Turnbull, and H. Ehrenreich (Academic, New York, 1968), Vol. 22, p. 1.

[11] J. M. Ziman, *Elements of Advanced Quantum Theory* (Cambridge University Press, Cambridge, 1969), p. 131.

[12] P. A. Wolff, Phys. Rev. **124**, 1030 (1961).

[13] A. M. Clogston, Phys. Rev. **125**, 439 (1962).

[14] P. B. Wiegmann, J. Phys. C: Solid State Phys. **14**, 1463 (1981).

[15] N. Andrei, K. Furuya, and J. H. Lowenstein, Rev. Mod. Phys. **55**, 331 (1983).

[16] M. A. Woodbury, Inverting modified matrices, Memorandum Report No. 42, Statistical Research Group, Princeton University, Princeton, 1950 (unpublished); see also https://en.wikipedia.org/wiki/Woodbury_matrix_identity.

[17] N. J. Stone, At. Data Nucl. Data Tables **90**, 75 (2005).

[18] E. N. Economou, *Green's Functions in Quantum Physics*, 3rd ed. (Springer, Berlin, 2006).

[19] W. Wiertz and R. R. Gerhardts, Z. Phys. B **25**, 19 (1976).

[20] K. Wildberger, P. Lang, R. Zeller, and P. H. Dederichs, Phys. Rev. B **52**, 11502 (1995).

[21] J. K. Furdyna, J. Appl. Phys. **64**, R29 (1988).

[22] B. Daniel, K. C. Agarwal, J. Lupaca-Schomber, C. Klingshirn, and M. Hetterich, Appl. Phys. Lett. **87**, 212103 (2005).

[23] J. Ravichandran, W. Siemons, M. L. Scullin, S. Mukerjee, M. Huijben, J. E. Moore, A. Majumdar, and R. Ramesh, Phys. Rev. B **83**, 035101 (2011).

[24] K. van Benthema, C. Elsasser, and R. H. French, J. Appl. Phys. **90**, 6156 (2001).

[25] M. S. S. Brooks, T. Gasche, S. Auluck, L. Nordstrom, L. Severin, J. Trygg, and B. Johansson, J. Appl. Phys. **70**, 5972 (1991).

[26] M. S. S. Brooks, in *Magnetism in Metals, A Symposium in Memory of Allan Mackintosh*, edited by D. F. McMorrow, J. Jensen, and H. M. Ronnow (The Royal Danish Academy of Sciences and Letters, Copenhagen, 1997), p. 291; see also https://www.fys.ku.dk/~jjensen/Book/Allansympc.pdf.

[27] The factor of 2 in $J_{4f\text{-}5d} = -J/(2\Omega_0)$ follows from other definition of the coupling constant used in Eq. (6) and Ref. [26] or Eq. (158).

[28] J. G. Kim, E. K. Lee, and S. Lee, Phys. Rev. B **51**, 670(R) (1995).

[29] W. Zawadzki, Adv. Phys. **23**, 435 (1974).

[30] M. G. Calkin, D. Kiang, and Y. Nogami, Am. J. Phys. **55**, 737 (1987).

[31] K. M. Case, Phys. Rev. **80**, 797 (1950).

[32] S. J. Frisken and D. J. Miller, Phys. Rev. Lett. **57**, 2971 (1986).

[33] P. Coleman, in *Many-Body Physics: From Kondo to Hubbard*, edited by E. Pavarini, E. Koch, and P. Coleman, (Forschungszentrum Jülich, Jülich, Germany, 2015), Chaps. 1, 1.1–1.34.

[34] P. G. de Gennes, J. Phys. Radium **23**, 630 (1962).

[35] L. N. Bulaevski and S. V. Panyukov, Pis'ma Zh. Eksp. Teor. Fiz. **43**, 190 (1986) [Sov. Phys. JETP Lett. **43**, 240 (1986)].

[36] T. M. Rusin and W. Zawadzki, Phys. Rev. B **97**, 205410 (2018).

[37] C. Proetto and A. Lopez, Phys. Rev. B **25**, 7037 (1982).

[38] Y. Yafet, Phys. Rev. B **36**, 3948 (1987).

[39] V. I. Litvinov and V. K. Dugaev, Phys. Rev. B **58**, 3584 (1998).

[40] T. M. Rusin and W. Zawadzki, J. Magn. Magn. Mater. **441**, 387 (2017).

[41] S. H. Liu, Phys. Rev. **121**, 451 (1961).

[42] P. D. Gorman, J. M. Duffy, S. R. Power, and M. S. Ferreira, Phys. Rev. B **90**, 125411 (2014).

[43] P. Lloyd, Proc. Phys. Soc. London **90**, 207 (1967); **90**, 217 (1967).